Non-covalent allosteric regulation of capsule catalysis

Supporting Information

Non-Covalent Allosteric Regulation of Capsule Catalysis

Vicente Martí-Centelles, Rebecca L. Spicer and Paul J. Lusby*

Table of Contents

Experimental Procedures

All reagents and solvents were purchased from Alfa Aesar, VWR or Sigma Aldrich and used without further purification unless stated otherwise. All reactions were carried out under air, unless stated otherwise. Benzoquinone was recrystallized form hot CH_2Cl_2/pet ether 60-80 (1:5). Cages **C-1** and **C-2** were prepared using literature procedures.[S1,S2]

All ^1H, ^{13}C and ^{19}F NMR spectra were recorded on either a 500 MHz Bruker AV III equipped with a DCH cryo-probe (Ava500), a 500 MHz Bruker AV IIIHD equipped with a Prodigy cryo-probe (Pro500), a 600 MHz Bruker AV IIIHD equipped with a TCI cryo-probe (Ava600) or a 400 MHz Bruker AV III equipped with BBFO+ probe (Ava400) at a constant temperature of 300 K. The temperature was set and controlled at 300 K with an air flow of 400 L h^{-1} in order to avoid any temperature fluctuations due to sample heating during the magnetic field pulse gradients. Chemical shifts are reported in parts per million. Coupling constants (J) are reported uncorrected in hertz (Hz). Apparent multiplicities are reported using the following standard abbreviations: m = multiplet, q = quartet, t = triplet, d = doublet, s = singlet, bs = broad singlet. All analysis was performed with MestReNova, Version 11. All assignments were made using a combination of COSY, NOESY, HSQC and HMBC NMR spectra.

All UV/Vis spectroscopy was carried out on a JASCO V-670 Spectrophotometer running Spectra Manager II (Jasco). All measurements were made at room temperature using a fused silica cuvette with a 10 mm path length, unless stated otherwise.

Initial host–guest experiments cage C-2 with Ph_3PO and benzoquinone

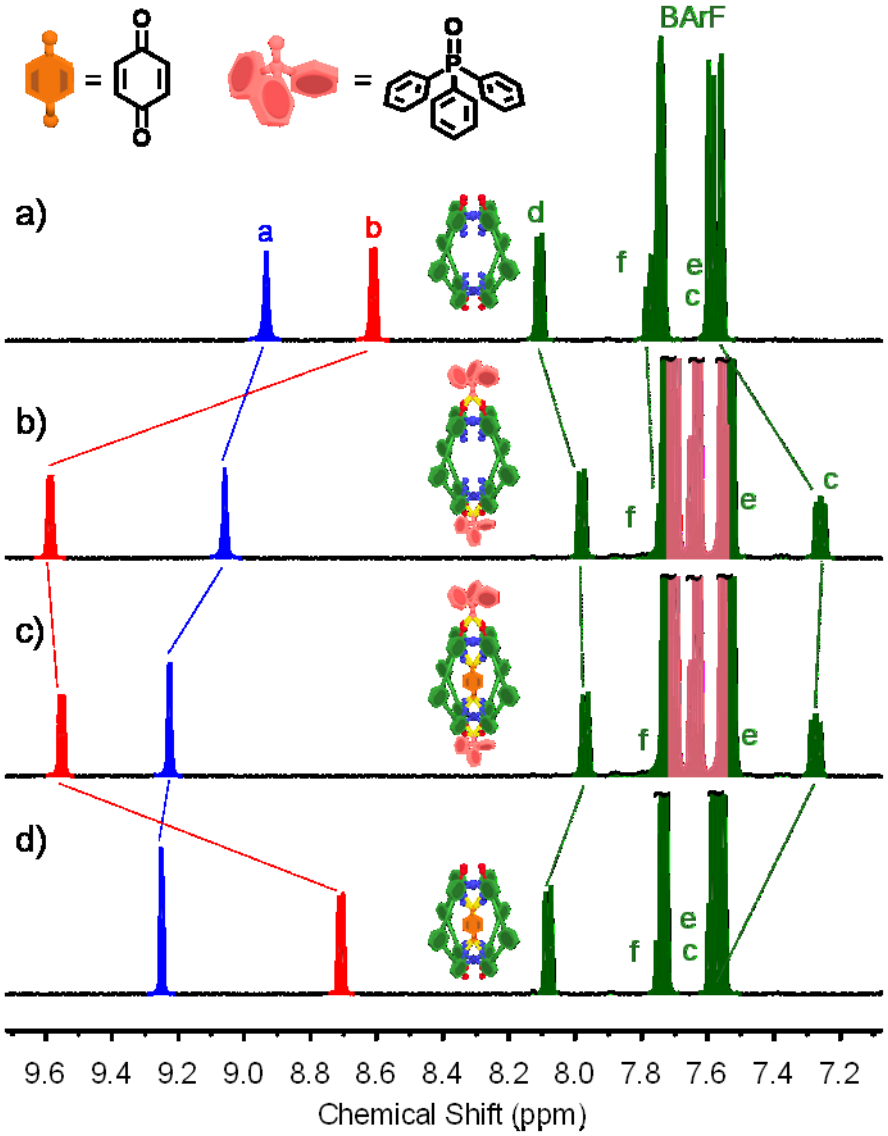

Figure S1. ^{1}H NMR (500 MHz, CD_2Cl_2, 300 K): (a) cage **C-2** (0.5 mM), (b) cage **C-2** (0.5 mM) and Ph_3PO (5 mM), (c) cage **C-2** (0.5 mM), Ph_3PO (5 mM) and benzoquinone (5 mM), (d) cage **C-2** (0.5 mM) and benzoquinone (5 mM).

Association constant determination

Experimental details

^{1}H NMR titration experiments were carried out on a 400 MHz Bruker AV III spectrometer equipped with BBFO+ probe (Ava400) at 300 K. Initial sample volumes were 500 µL with 0.45–0.50 mM concentration of the cage (**C-1** or **C-2**). Solutions of the guest quinones were 15–30 mM in the same stock solution of the cage. ^{1}H NMR spectra were recorded at 0–30 equivalents of quinone.

All UV/Vis spectroscopy titration experiments were carried out on a JASCO V-670 Spectrophotometer running Spectra Manager II (Jasco). All measurements were made at room temperature using a fused silica cuvette with a 10 mm path length. Initial sample volumes were 2000 µL with 10–50 µM concentration of pentacenequinone. Solutions of the cage (**C-1** or **C-2**) were 0.2–1 mM in the same stock solution of the pentacenequinone. UV-Vis spectra were recorded at 0–2.5 equivalents of pentacenequinone. For experiments with Ph_3PO a very similar procedure was used: initial sample volumes were 2000 µL with 10–50 µM concentration of pentacenequinone and Ph_3PO 1–5 mM. Solutions of the cage (**C-1** or **C-2**) were 0.2–1 mM in the same stock solution of the pentacenequinone with Ph_3PO. UV-Vis spectra were recorded at 0–2.5 equivalents of cage.

Association constants were obtained by analysis of the resulting titration data and fitting to the models described below using the Levenberg-Marquardt Nonlinear Least-Squares Algorithm[S3] implemented in the R software[S4] and the RStudio[S5] software interface. The error of the determined association constants are estimated to be less than 10%.

Models of the host-guest complexes

For each host-guest complex considered in this work the corresponding equations[S6] associated to the equilibrium system (described in this section) were be solved numerically using the R software (*nleqslv* library for multiple equation solving)[S7] except for the 1:1 host–guest model where the corresponding algebraic equation was used.[2,6]

Host–Guest 1:2 [Cage·(Ph_3PO)$_2$]

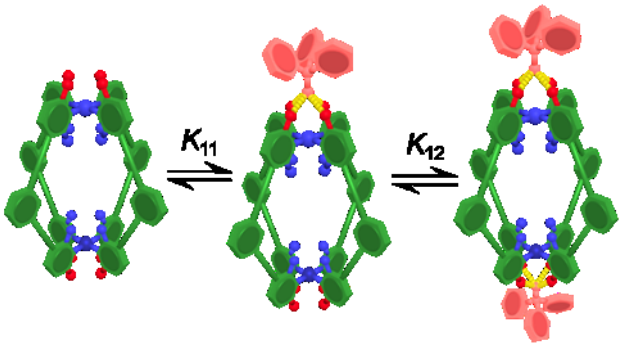

Figure S2. Equilibria involved in the binding of Ph_3PO in the outside binding pockets of the cage.

The corresponding equations for the equilibria represented in the Figure S2 are:

$[Host]_0 = [H] + [HG] + [HG_2]$

$[Guest]_0 = [G] + [HG] + 2\,[HG_2]$

$K_{11} = [HG]/([H]\,[G])$

$K_{12} = [HG_2]/([HG]\,[G])$

For a system where the two sites behave independently (i.e. statistical 1:2 model) the system can be described with 3 parameters (K_{11}, δ_0 and δ_{12}) as long as $K_{11} = 4\times K_{12}$ and $\delta_{11} = (\delta_0 + \delta_{12})/2$.

It is important to note that a fast equilibrium is observed with regard to the ^{1}H NMR timescale and therefore time averaged spectra of this equilibrium can be described using the following equation:

$\delta = \delta_0\,([H]/[Host]_0) + \delta_{11}\,([HG]/[Host]_0) + \delta_{12}\,([HG_2]/[Host]_0)$

Fitting of the equation to the experimental data it was possible to obtain the K_{11} and K_{12} for Ph_3PO with both cages **C-1** and **C-2**.

The statistical 1:2 model is equivalent to the 1:1 binding model where the total binding sites concentration is twice the host concentration. The intrinsic association constant (K_{Ass}) can be obtained using the 1:1 model for fitting and 2 times concentration of the cage as the concentration of the host. For this fitting, the K_{11} and K_{12} are related with K_{Ass} by the statistical factors $\Omega_i = 2$ and $\Omega_i = 1/2$, and therefore $K_{11} = 2\times K_{Ass}$ and $K_{12} = 1/2\times K_{Ass}$ (see Figure S3).[S8] In both titrations of cages **C-1** and **C-2** with Ph_3PO the data fitted well to the 1:1 model (see Figure S7 and Figure S12).

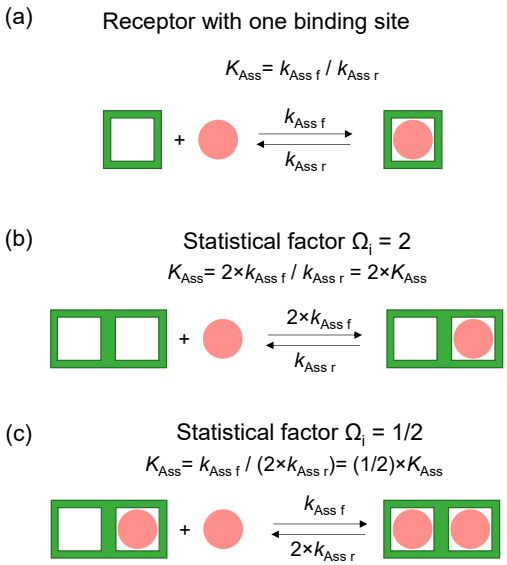

Figure S3. Statistical factors for the host–guest 1:2 binding model. (a) Host with one binding site, (b) Host with two binding sites, first association constant step of a receptor with two binding sites, (c) Host with one binding sites, second association constant step of a receptor with two binding sites.

External pockets Host–Guest 1:2 and internal cavity 1:1 guest binding for [(pentacenequinone⊂cage)·$(Ph_3PO)_2$]

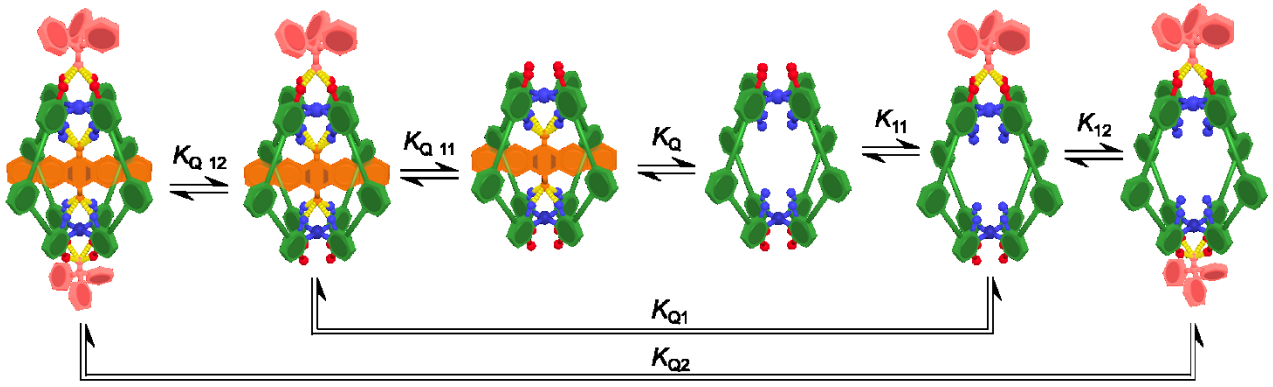

Figure S4. Equilibria involved in the cage–quinone–Ph_3PO system.

The corresponding mass balances and equilibrium constants are as follows (G1 = quinone, G2 = Ph_3PO, H = Host):

$[Host]_0 = [H] + [H{\cdot}G2] + [H{\cdot}(G2)_2] + [H{\cdot}G2{\cdot}G1] + [H{\cdot}(G2)_2{\cdot}G1] + [H{\cdot}G1]$

$[Guest1]_0 = [G2] + [H{\cdot}G2] + 2\,[H{\cdot}(G2)_2] + [H{\cdot}G2{\cdot}G1] + 2\,[H{\cdot}(G2)_2{\cdot}G1]$

$[Guest2]_0 = [G1] + [H{\cdot}G1] + [H{\cdot}G2{\cdot}G1] + [H{\cdot}(G2)_2{\cdot}G1]$

$K_{11} = [H{\cdot}G2]/([H]\,[G2])$

$K_{12} = [H{\cdot}(G2)_2]/([H{\cdot}G2]\,[G2])$

$K_{H{\cdot}G2{\cdot}G1} = [H{\cdot}G2{\cdot}G1]/([H{\cdot}G2]\,[G1])$

$K_{H{\cdot}(G2)_2{\cdot}G1} = [H{\cdot}(G2)_2{\cdot}G1]/([H{\cdot}(G2)_2]\,[G1])$

In these equilibria, ^{1}H NMR titration experiments indicate that both external sites behave independently in the absence and presence of the guest (see Figure S9), and therefore $K_{11} = 4{\times}K_{12}$ and $K_{Q11} = 4{\times}K_{Q12}$. Additionally, choosing a guest that binds in the internal cavity very strongly would allow to assume that $K_Q = K_{Q1} = K_{Q2} > 10^6$ M^{-1} (as confirmed by UV-Vis titrations, see UV-Vis titration section).

This complex set of equations was considered could not be used for benzoquinone guest that is in fast equilibrium with regard to the ^{1}H NMR timescale. For Ph_3PO guest under the experimental conditions using 0.5 mM cage **C-1** or **C-2** and 10 equivalents of Ph_3PO he calculated composition in solution is: 89% of 1:2 complex, 11% of 1:1 complex and less than 1% of free cage. Assuming only the major species in solution the association constant of benzoquinone with cages **C-1**·$(Ph_3PO)_2$ and **C-2**·$(Ph_3PO)_2$ using the standard host–guest 1:1 model used previously in our research group for cages **C-1** and **C-2** with quinone guests.[S2] The association constant of pentacenequinone with cage **C-1** is described in ref [S1] and the association constant of pentacenequinone with cage **C-2** is described in ref [S9].

For pentacenequinone guest the equilibria K_Q is in slow exchange with regard to the ^{1}H NMR timescale, and therefore, the change of the free cage signals with the addition Ph_3PO and [pentacenequinone⊂cage] with the addition of Ph_3PO could be monitored simultaneously in the same experiment. Simultaneous fitting was performed to obtain K_{11}, K_{12} for free cage and K_{Q11}, K_{Q12} for [pentacenequinone⊂cage] using the following equations:

$$\delta_H = \delta_{H0}\,([H]/([H]+[H\cdot G2]+[H\cdot(G2)_2])) + \delta_{H11}\,([H\cdot G2]/([H]+[H\cdot G2]+[H\cdot(G2)_2]))$$
$$+ \delta_{H12}\,([H\cdot(G2)_2]/([H]+[H\cdot G]+[H\cdot(G2)_2]))$$

$$\delta_{HQ} = \delta_{HG10}\,([H\cdot G1]/([H\cdot G1]+[H\cdot G1\cdot G2]+[H\cdot G1\cdot(G2)_2]))$$
$$+ \delta_{HG11}\,([H\cdot G1\cdot G2]/([H\cdot G1]+[H\cdot G1\cdot G2]+[H\cdot G1\cdot(G2)_2]))$$
$$+ \delta_{HG12}\,([H\cdot G1\cdot(G2)_2]/([H\cdot G1]+[H\cdot G1\cdot G2]+[H\cdot G1\cdot(G2)_2]))$$

Individual NMR titration data

Triphenylphosphine oxide with cage **C-1**

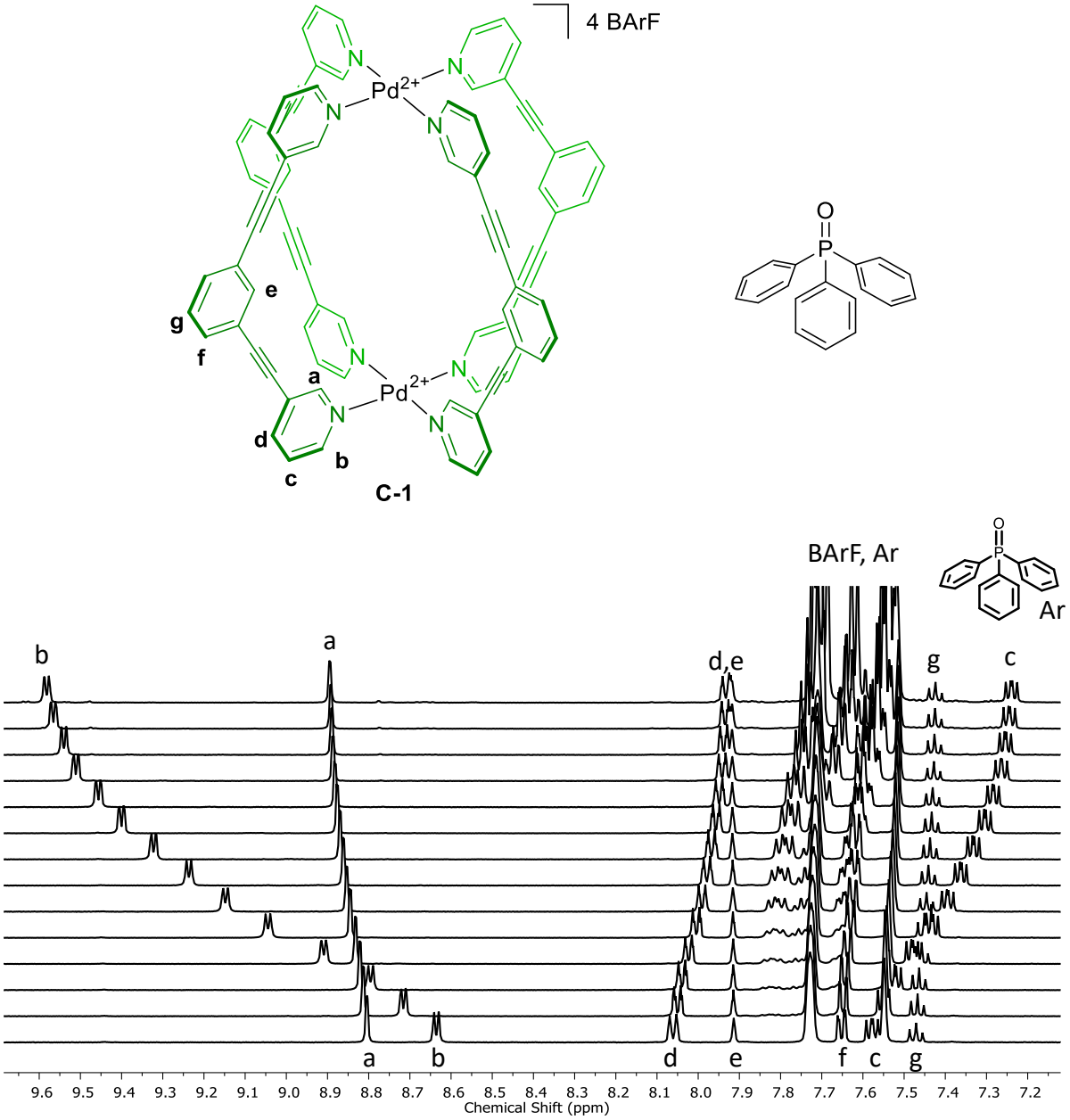

Figure S5. Partial ^{1}H NMR spectra (500 MHz, CD_2Cl_2, 300 K) of the titration of cage **C-1** (0.43 mM) with Ph_3PO (25 mM).

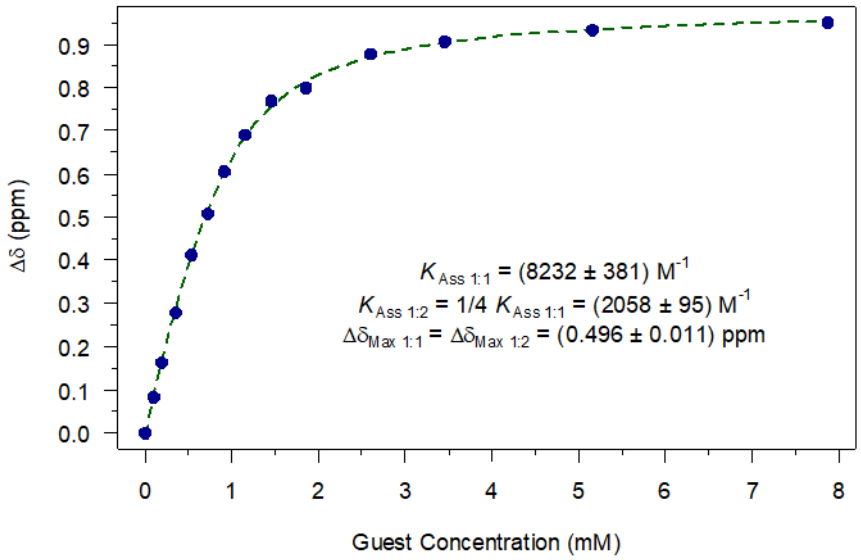

Figure S6. ^{1}H NMR (500 MHz, CD_2Cl_2, 300 K) titration curve of cage **C-1** (0.43 mM) with Ph_3PO (25 mM). Curve obtained by monitoring the external cage cavity proton *b*. The solid points represent experimental data and the continuous dashed line represents the fitted binding isotherm to the statistical 1:2 host–guest model.

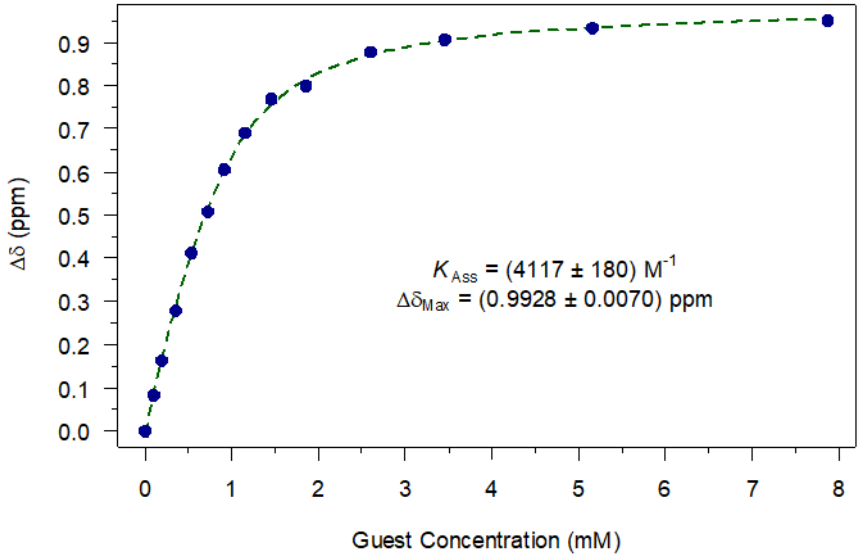

Figure S7. ^{1}H NMR (500 MHz, CD_2Cl_2, 300 K) titration curve of cage **C-1** (0.43 mM) with Ph_3PO (25 mM). Curve obtained by monitoring the external cage cavity proton *b*. The solid points represent experimental data and the continuous dashed line represents the fitted binding isotherm to the 1:1 host–guest model using [Host]. = 2×[**C-1**] = 0.86 mM, therefore $K_{11} = 2\times K_{Ass} = 2 \times 4117\ M^{-1} = 8234\ M^{-1}$ and $K_{12} = 1/2\times K_{Ass} = 1/2 \times 4117\ M^{-1} = 2059\ M^{-1}$.

Triphenylphosphine oxide simultaneously with [pentacenequinone ⊂**C-1**] and **C-1**

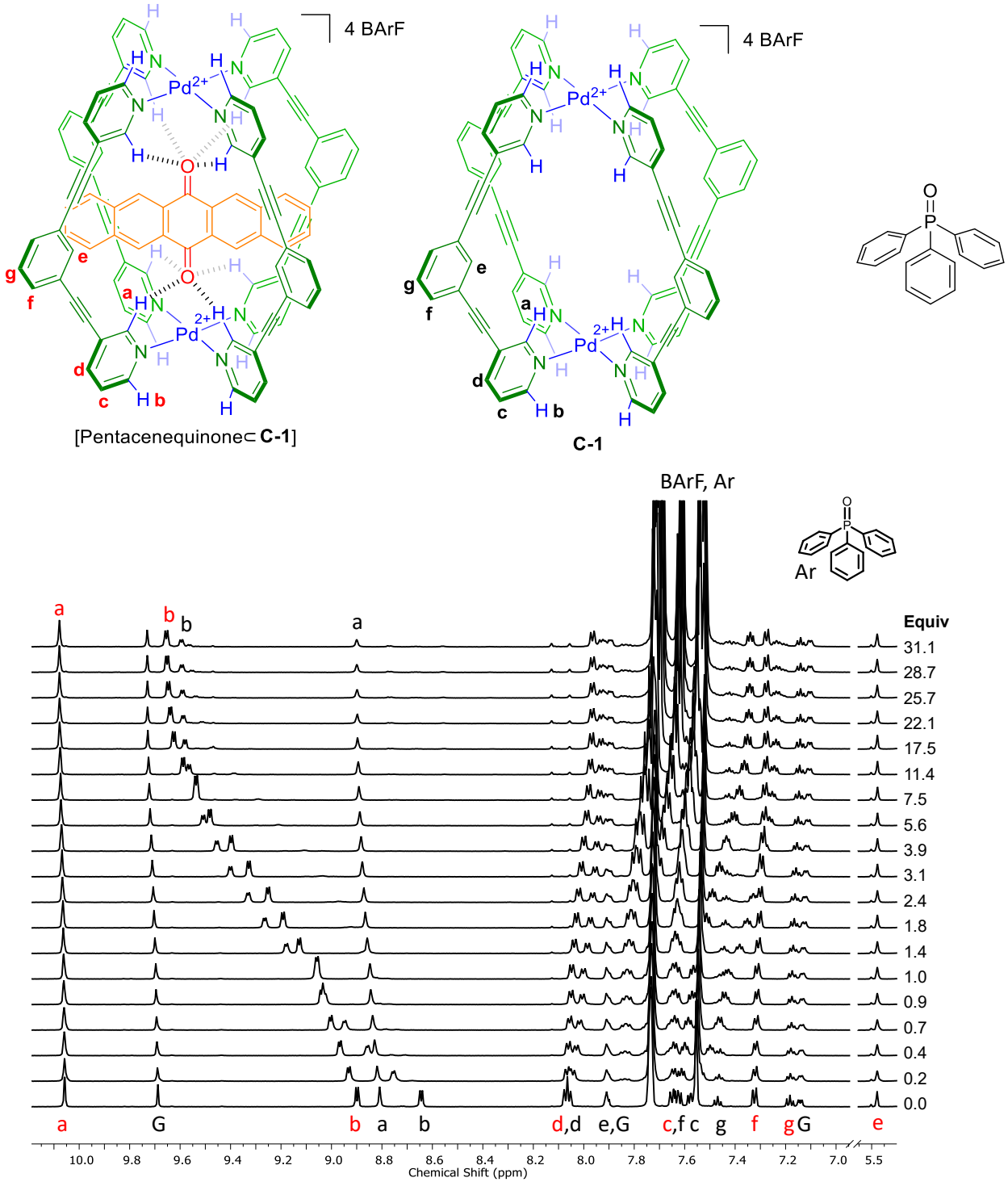

Figure S8. Partial ^{1}H NMR spectra (600 MHz, CD_2Cl_2, 300 K) of the titration of cage **C-1** (0.48 mM) in the presence of pentacenequinone (0.25 mM) with Ph_3PO.

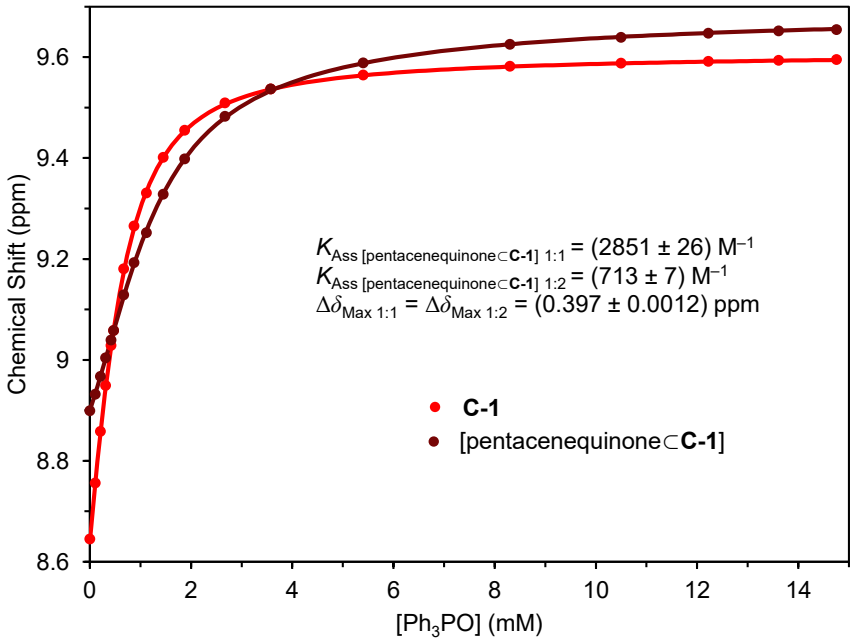

Figure S9. ^{1}H NMR (600 MHz, CD_2Cl_2, 300 K) titration curve of cage **C-2** (0.47 mM) in the presence of pentacenequinone (0.25 mM) with Ph_3PO (25 mM). Curves obtained by monitoring the external cage cavity proton *b* for empty cage (red) and [pentacenequinone⊂**C-1**] (brown). The solid points represent experimental data, the continuous brown line represents the fitted binding isotherm, and the continuous red line represents the predicted binding isotherm using the previously determined association constants for cage only.

Triphenylphosphine oxide with cage **C-2**

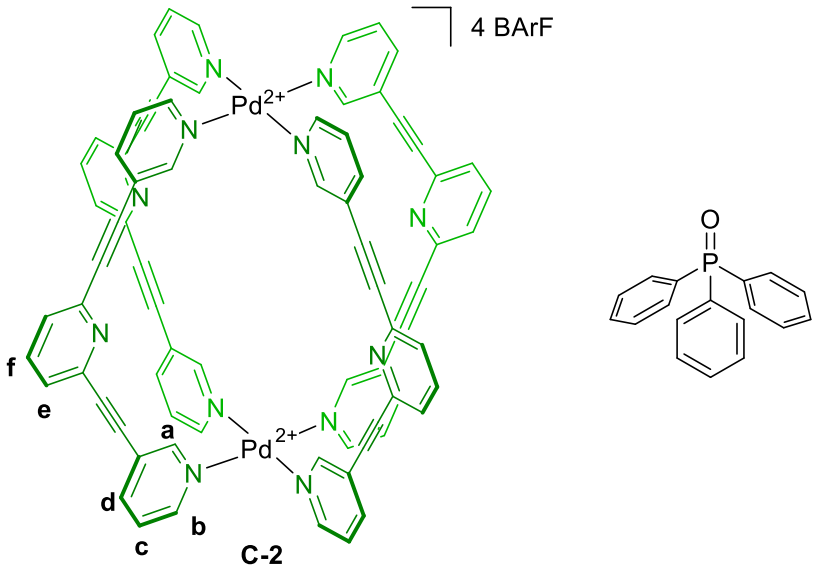

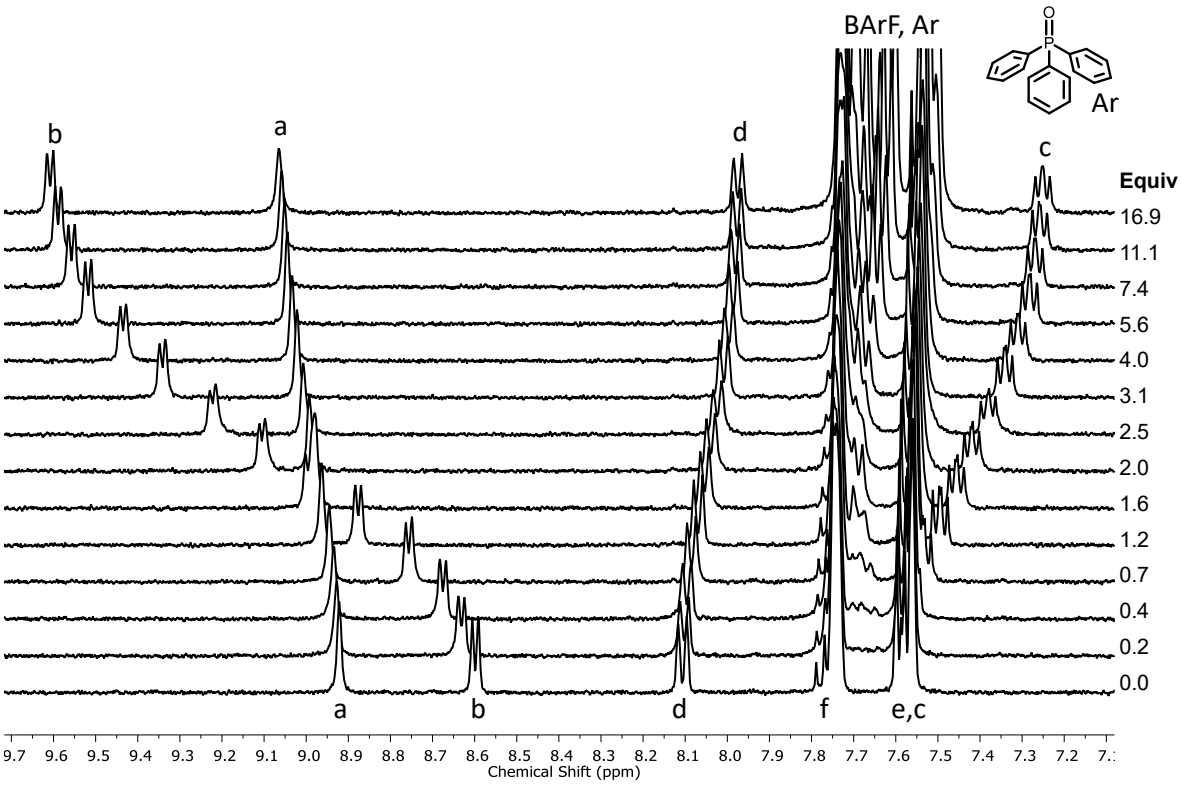

Figure S10. Partial ^{1}H NMR spectra (400 MHz, CD_2Cl_2, 300 K) of the titration of cage **C-2** (0.47 mM) with Ph_3PO (25 mM).

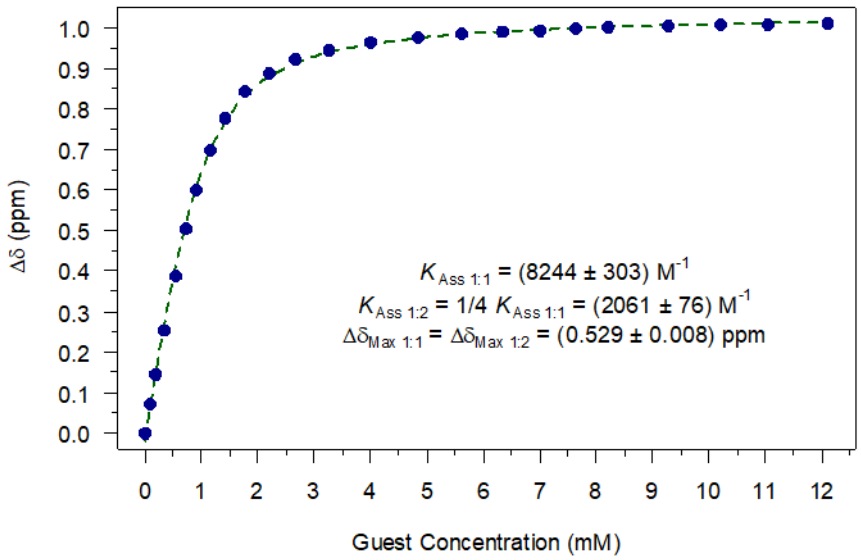

Figure S11. ^{1}H NMR (400 MHz, CD_2Cl_2, 300 K) titration curve of cage **C-2** (0.47 mM) with Ph_3PO (25 mM). Curve obtained by monitoring the external cage cavity proton *b*. The solid points represent experimental data and the continuous dashed line represents the fitted binding isotherm to the statistical 1:2 host–guest model.

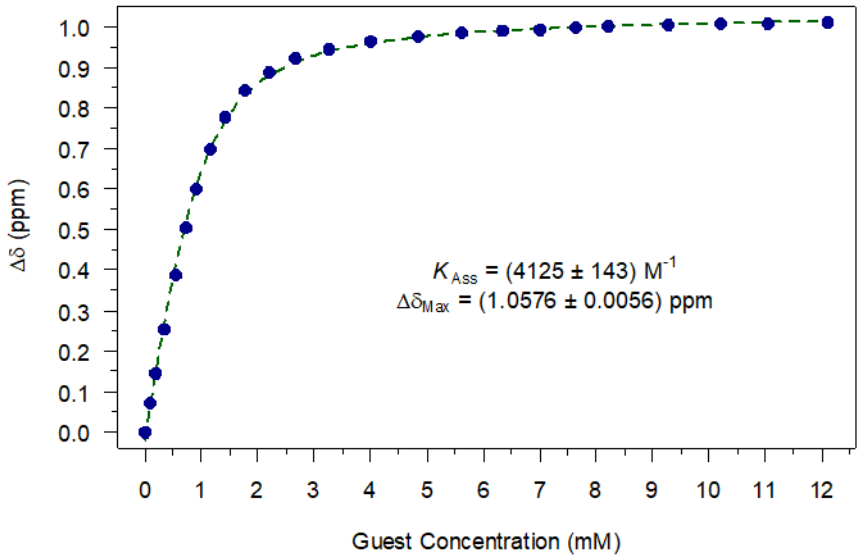

Figure S12. ^{1}H NMR (400 MHz, CD_2Cl_2, 300 K) titration curve of cage **C-2** (0.47 mM) with Ph_3PO (25 mM). Curve obtained by monitoring the external cage cavity proton *b*. The solid points represent experimental data and the continuous dashed line represents the fitted binding isotherm to the 1:1 host–guest model using [Host]. = 2×[**C-2**] = 0.94 mM, therefore $K_{11} = 2\times K_{Ass} = 2 \times 4125\ M^{-1} = 8250\ M^{-1}$ and $K_{12} = 1/2\times K_{Ass} = 1/2 \times 4125\ M^{-1} = 2063\ M^{-1}$.

Triphenylphosphine oxide with [*N*-methylmaleimide⊂**C-1**]

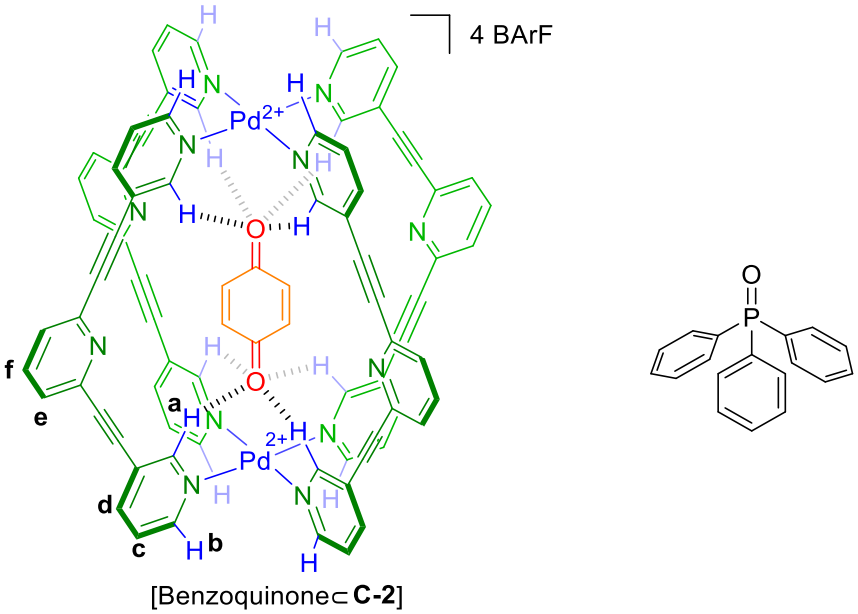

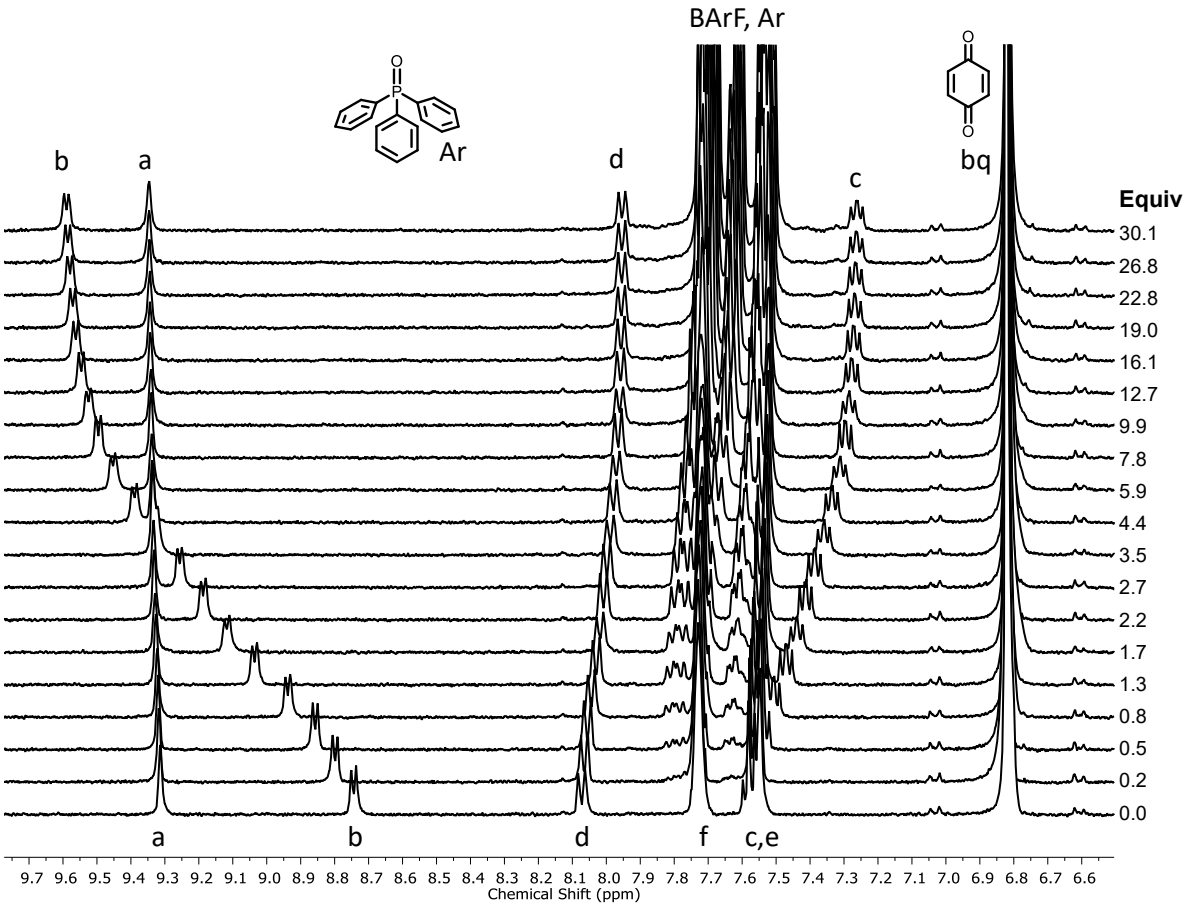

Figure S13. Partial ^{1}H NMR spectra (400 MHz, CD_2Cl_2, 300 K) of the titration of cage **C-2** (0.42 mM) in the presence of benzoquinone (25 mM) with Ph_3PO (25 mM).

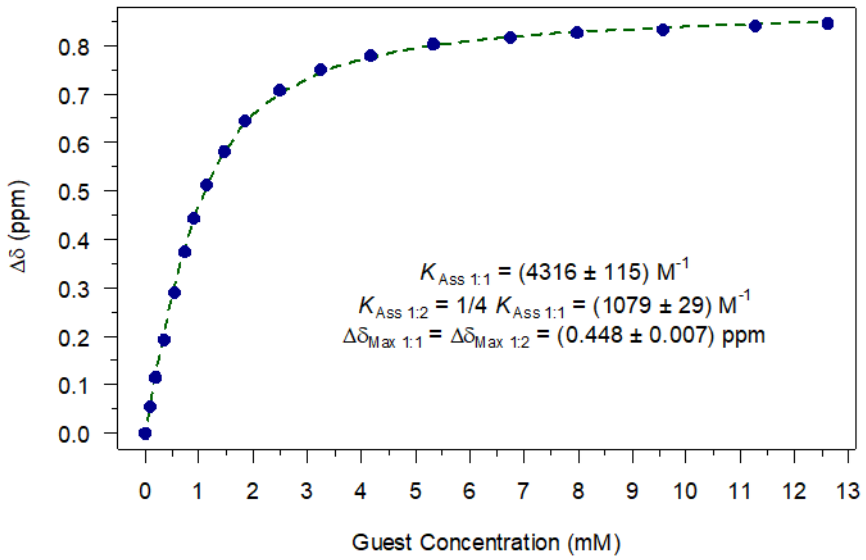

Figure S14. ^{1}H NMR (400 MHz, CD_2Cl_2, 300 K) titration curve of cage **C-2** (0.42 mM) in the presence of benzoquinone (25 mM) with Ph_3PO (25 mM). Curve obtained by monitoring the external cage cavity proton *b*. The solid points represent experimental data and the continuous dashed line represents the fitted binding isotherm to the statistical 1:2 host–guest model.

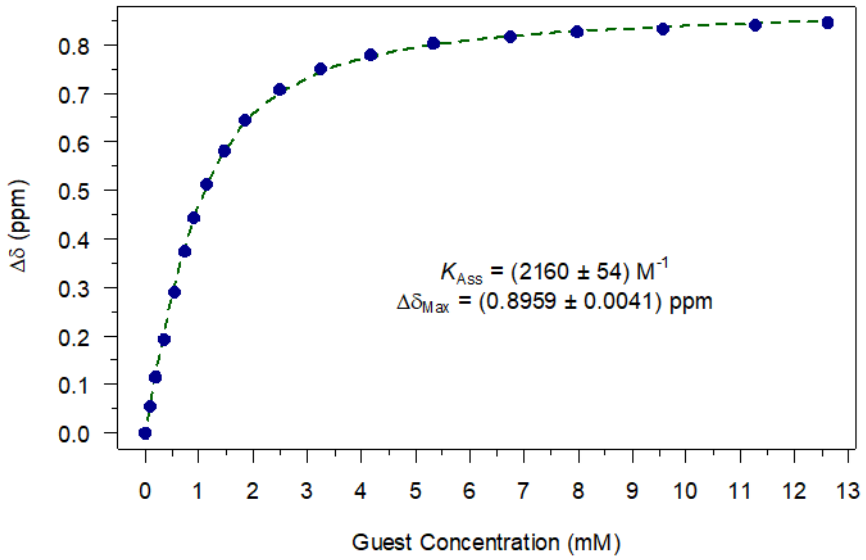

Figure S15. ^{1}H NMR (400 MHz, CD_2Cl_2, 300 K) titration curve of cage **C-2** (0.42 mM) in the presence of benzoquinone (25 mM) with Ph_3PO (25 mM). Curve obtained by monitoring the external cage cavity proton *b*. The solid points represent experimental data and the continuous dashed line represents the fitted binding isotherm to the 1:1 host–guest model using [Host]. = 2×[**C-2**] = 0.84 mM, therefore $K_{11} = 2\times K_{Ass} = 2 \times 2160\ M^{-1} = 4320\ M^{-1}$ and $K_{12} = 1/2\times K_{Ass} = 1/2 \times 2160\ M^{-1} = 1080\ M^{-1}$.

Benzoquinone with [**C-1**·$(Ph_3PO)_2$]

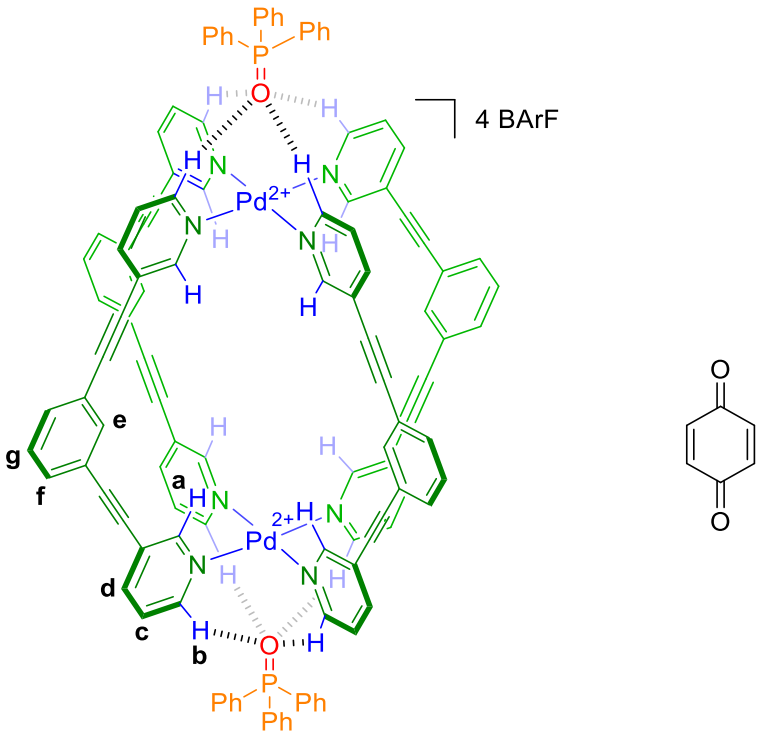

[**C-1**·$(Ph_3PO)_2$]

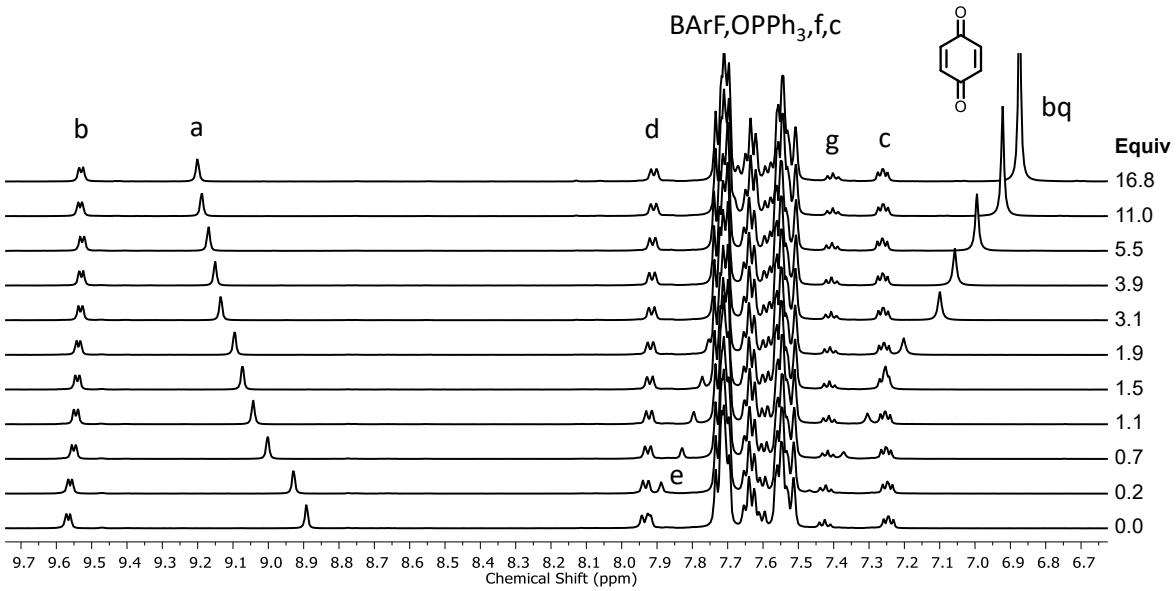

Figure S16. Partial ^{1}H NMR spectra (500 MHz, CD_2Cl_2, 300 K) of the titration of cage **C-1** (0.47 mM) with benzoquinone (25 mM) in the presence of Ph_3PO (5 mM).

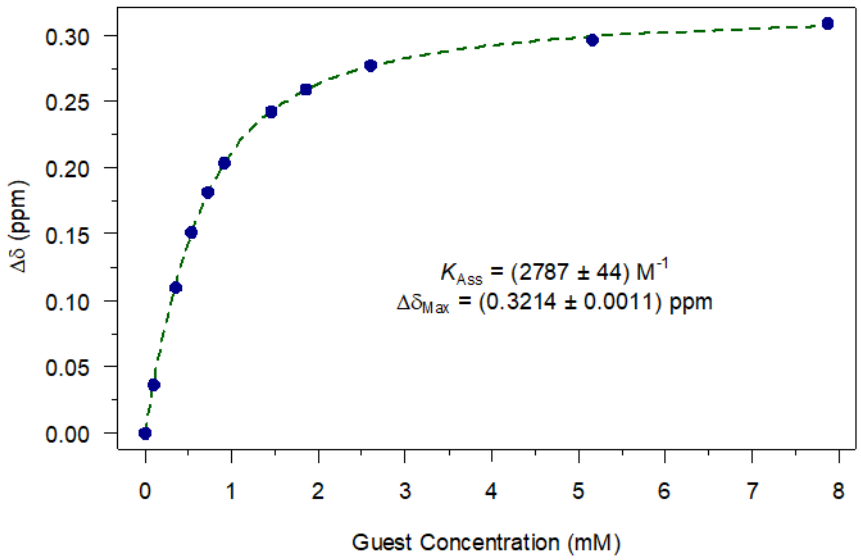

Figure S17. ^{1}H NMR (500 MHz, CD_2Cl_2, 300 K) titration curve of cage **C-1** (0.47 mM) with benzoquinone (25 mM) in the presence of Ph_3PO (5 mM). Curve obtained by monitoring the internal cage cavity proton *a*. The solid points represent experimental data and the continuous dashed line represents the fitted binding isotherm to the model host–guest 1:1.

Benzoquinone with [**C-2**·$(Ph_3PO)_2$]

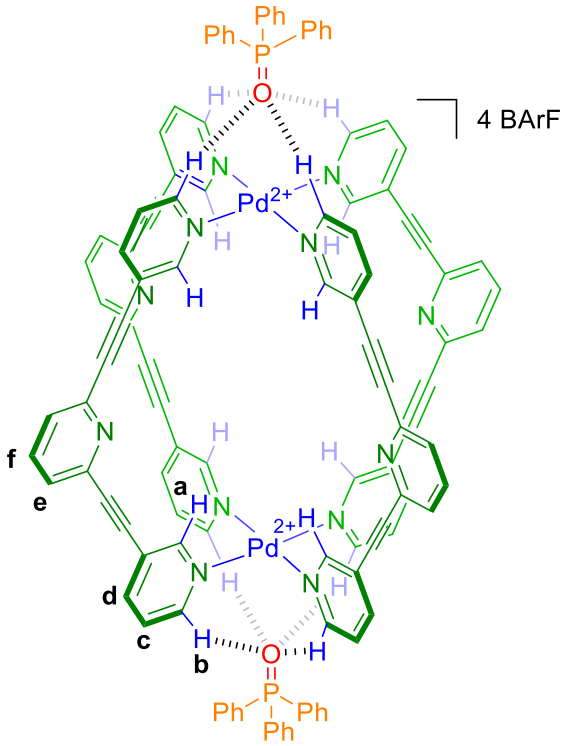

[**C-2**·$(Ph_3PO)_2$]

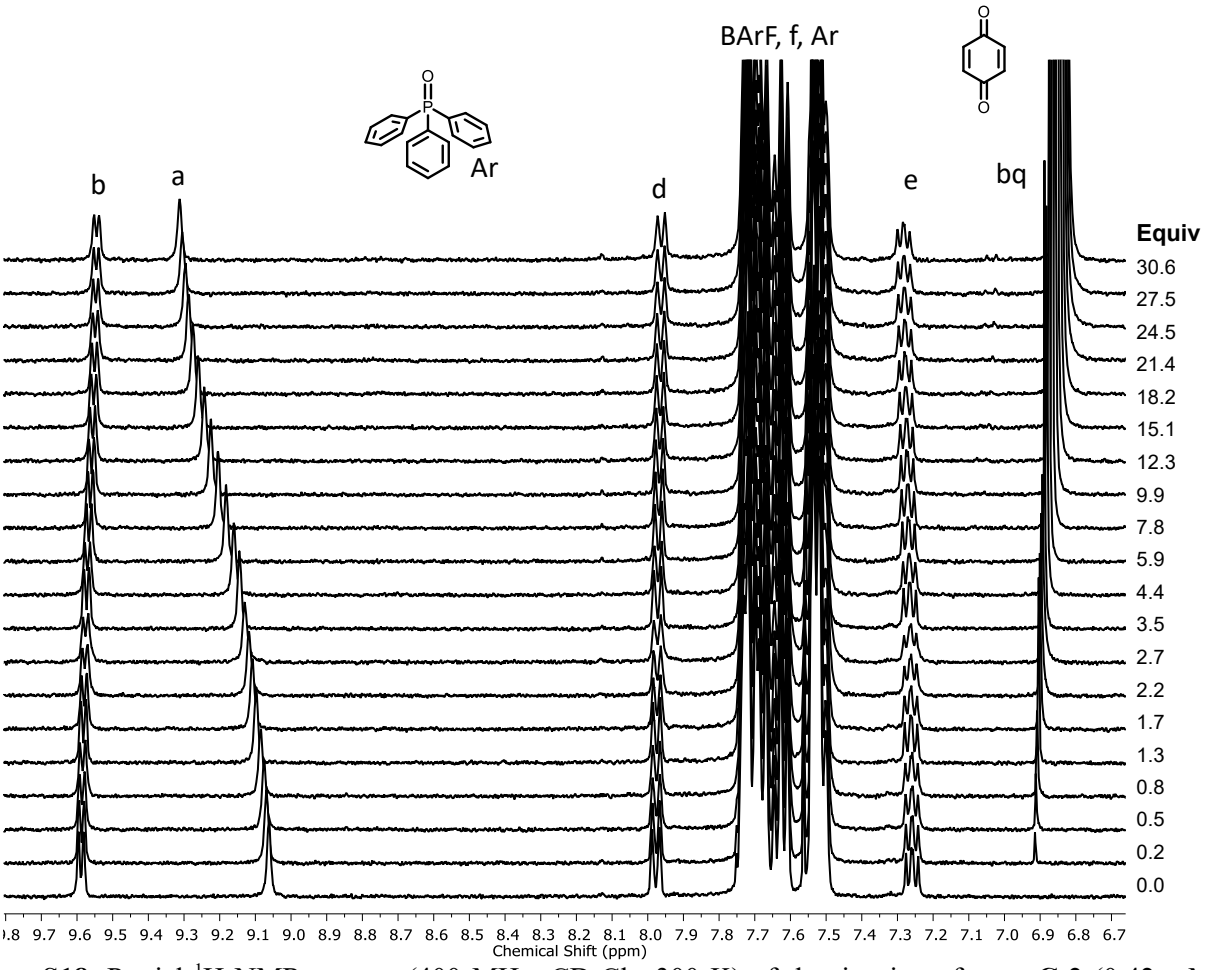

Figure S18. Partial ^{1}H NMR spectra (400 MHz, CD_2Cl_2, 300 K) of the titration of cage **C-2** (0.42 mM) with benzoquinone (25 mM) in the presence of Ph_3PO (5 mM).

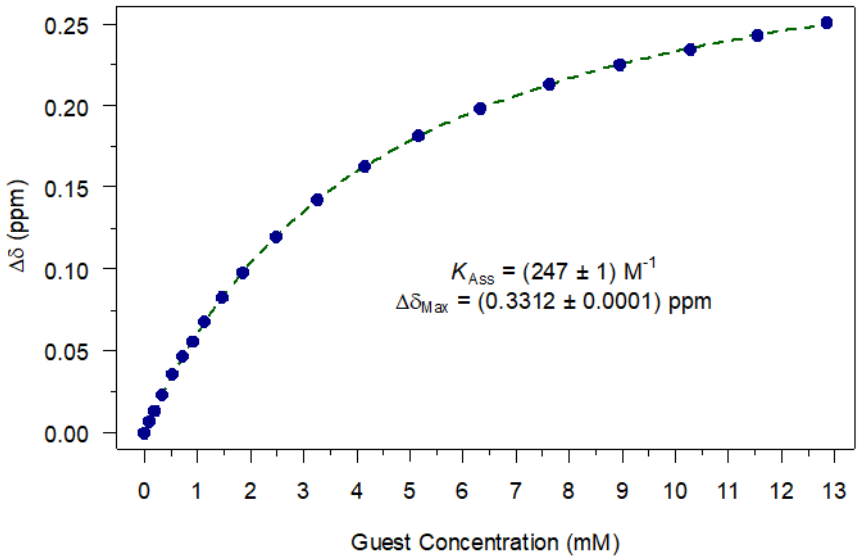

Figure S19. ^{1}H NMR (400 MHz, CD_2Cl_2, 300 K) titration curve of cage **C-2** (0.42 mM) with benzoquinone (25 mM) in the presence of Ph_3PO (5 mM). Curve obtained by monitoring the internal cage cavity proton *a*. The solid points represent experimental data and the continuous dashed line represents the fitted binding isotherm to the model host–guest 1:1.

Individual UV-Vis titration data

Pentacenequinone with cage **C-1**

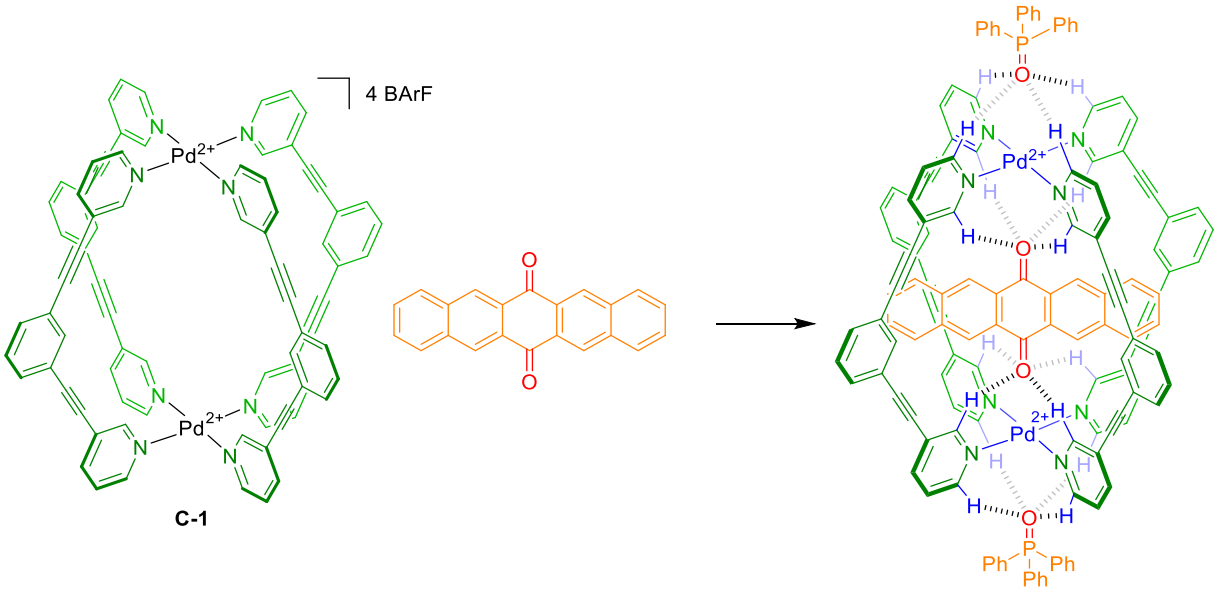

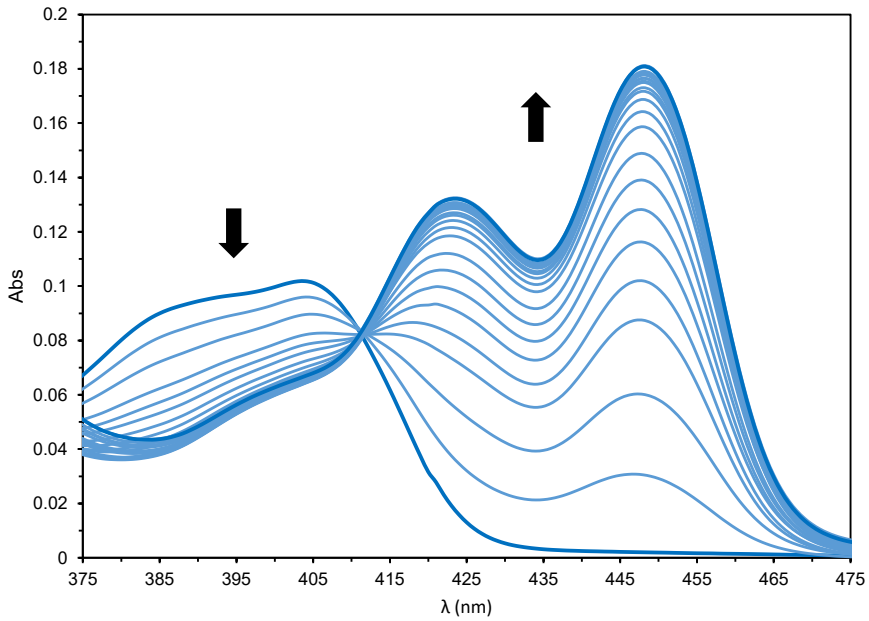

Figure S20. UV-Vis (CH_2Cl_2, rt) of the titration of pentacenequinone (10 μM) with cage **C-1** (0 to 2.3 equiv).

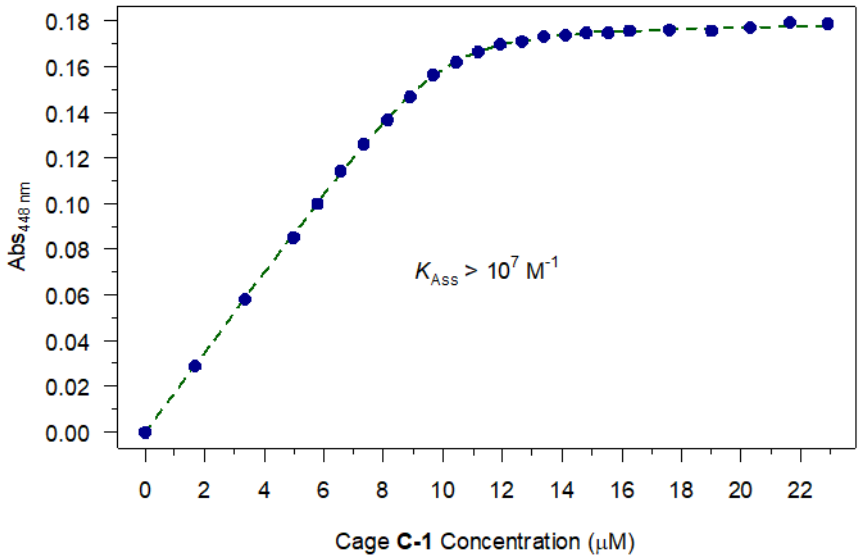

Figure S21. UV-Vis (CH_2Cl_2, rt) titration curve of pentacenequinone (10 μM) with cage **C-1** (0 to 2.3 equiv). Curve obtained by monitoring the absorbance at 447 nm. The solid points represent experimental data and the continuous dashed line represents the fitted binding isotherm to the model host–guest 1:1.

Pentacenequinone with cage [**C-1**·(Ph_3PO)]

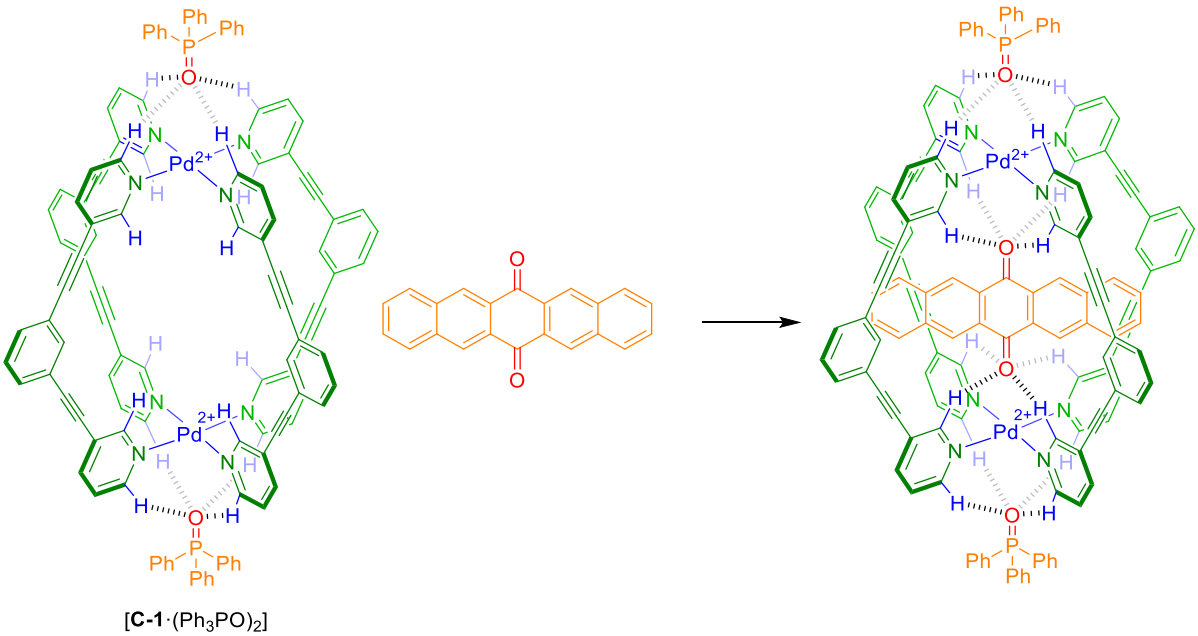

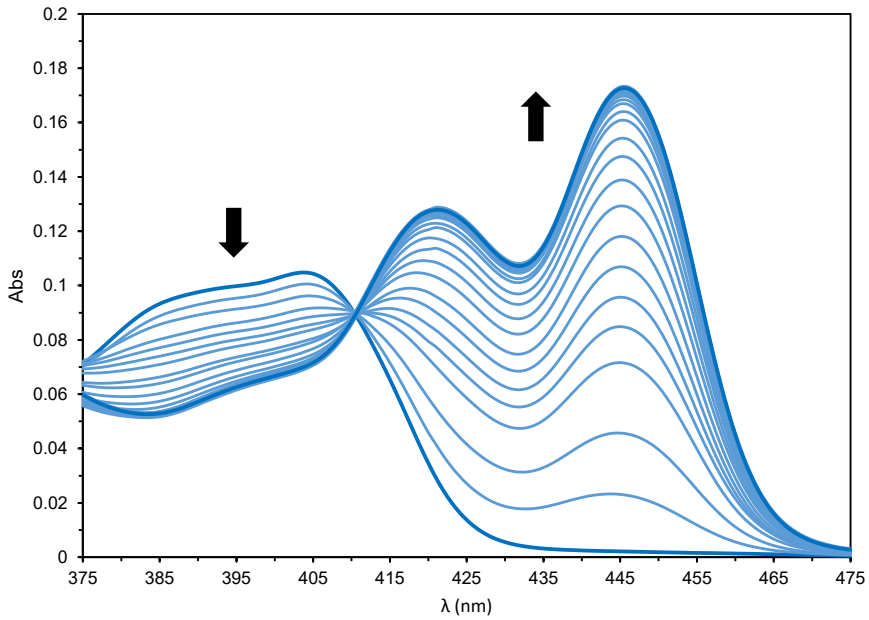

Figure S22. UV-Vis (CH_2Cl_2, rt) of the titration of pentacenequinone (10 μM) with cage **C-1** (0 to 2.0 equiv) in the presence of Ph_3PO (1 mM).

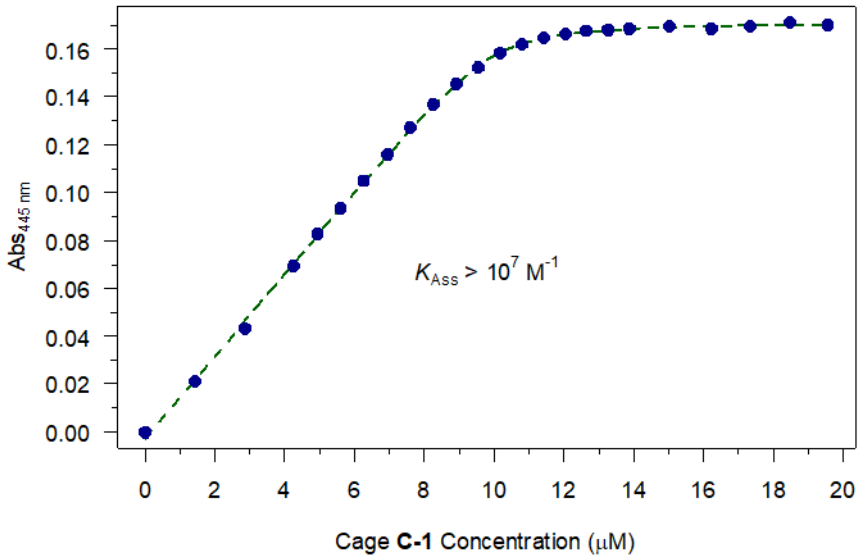

Figure S23. UV-Vis (CH_2Cl_2, rt) titration curve of pentacenequinone (10 μM) with cage **C-1** (0 to 2.0 equiv) in the presence of Ph_3PO (1 mM). Curve obtained by monitoring the absorbance at 444 nm. The solid points represent experimental data and the continuous dashed line represents the fitted binding isotherm to the model host–guest 1:1. Under these conditions the estimated species distribution using the $K_{Ass\ \mathbf{C\text{-}1}\text{–}(Ph_3PO)_2}$ = 8200 M^{-1} and $K_{Ass\ \mathbf{C\text{-}1}\text{–}Ph_3PO}$ = 2100 M^{-1} is: 4% free cage **C-1**, 31% **C-1**(Ph_3PO) complex, and 65% **C-1**($Ph_3PO)_2$ complex.

Pentacenequinone with cage [**C-2**·(Ph_3PO)]

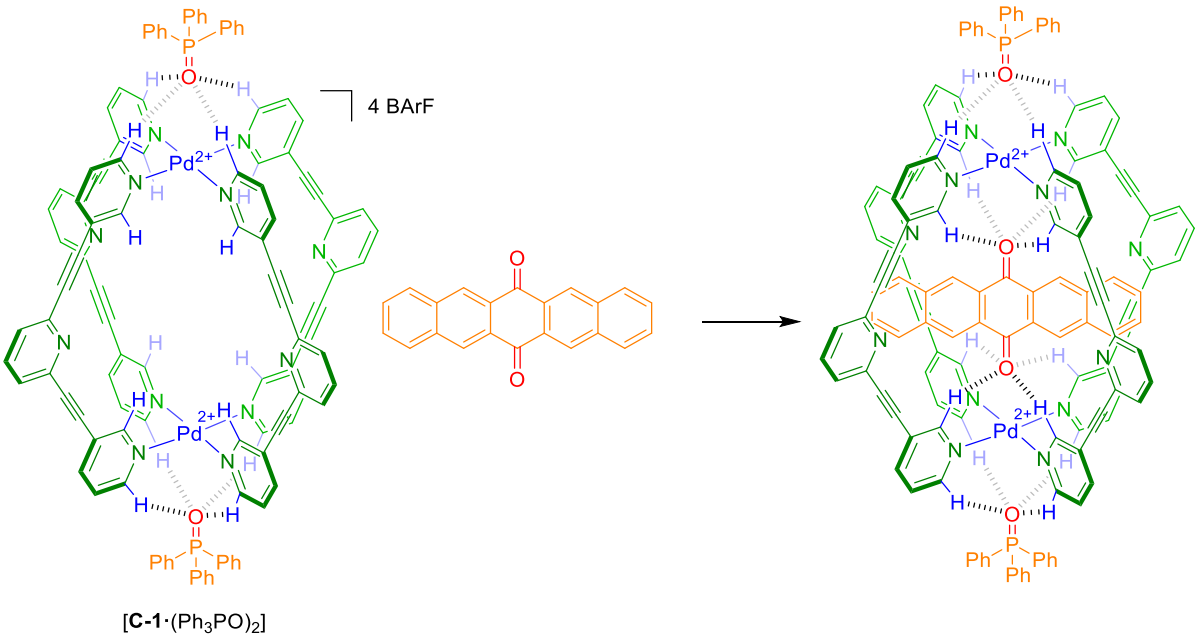

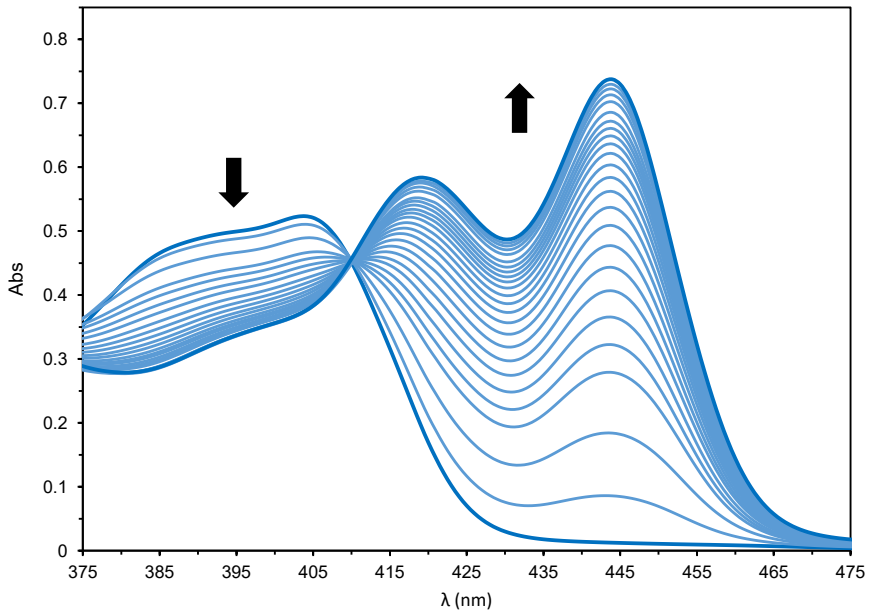

Figure S24. UV-Vis (CH_2Cl_2, rt) of the titration of pentacenequinone (50 μM) with cage **C-2** (0 to 2.0 equiv) in the presence of Ph_3PO (5 mM).

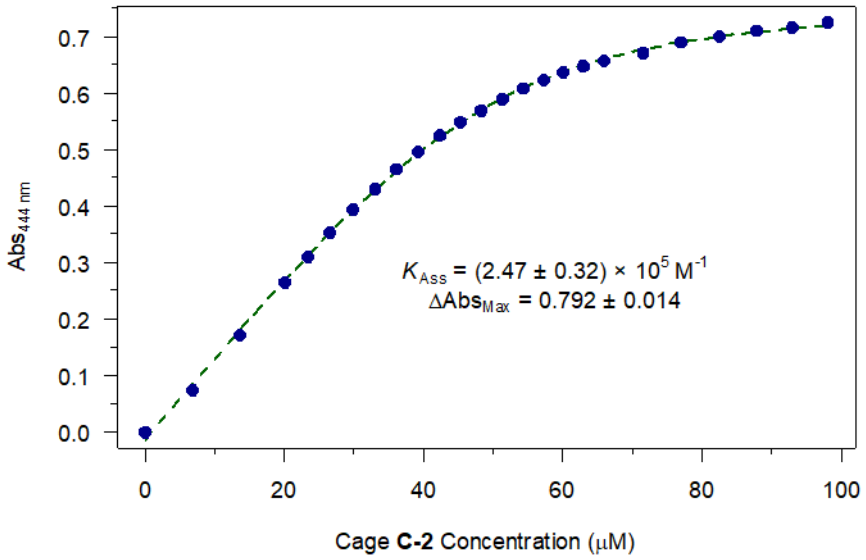

Figure S25. UV-Vis (CH_2Cl_2, rt) titration curve of pentacenequinone (50 μM) with cage **C-2** (0 to 2.0 equiv) in the presence of Ph_3PO (5 mM). Curve obtained by monitoring the absorbance at 444 nm. The solid points represent experimental data and the continuous dashed line represents the fitted binding isotherm to the model host–guest 1:1. Under these conditions the estimated species distribution using the $K_{Ass\ \mathbf{C\text{-}2}\text{–}(Ph_3PO)_2}$ = 8200 M^{-1} and $K_{Ass\ \mathbf{C\text{-}2}\text{–}Ph_3PO}$ = 2100 M^{-1} is: <1% free cage **C-2**, 9% **C-1**(Ph_3PO) complex, and 91% **C-1**(Ph_3PO)$_2$ complex.

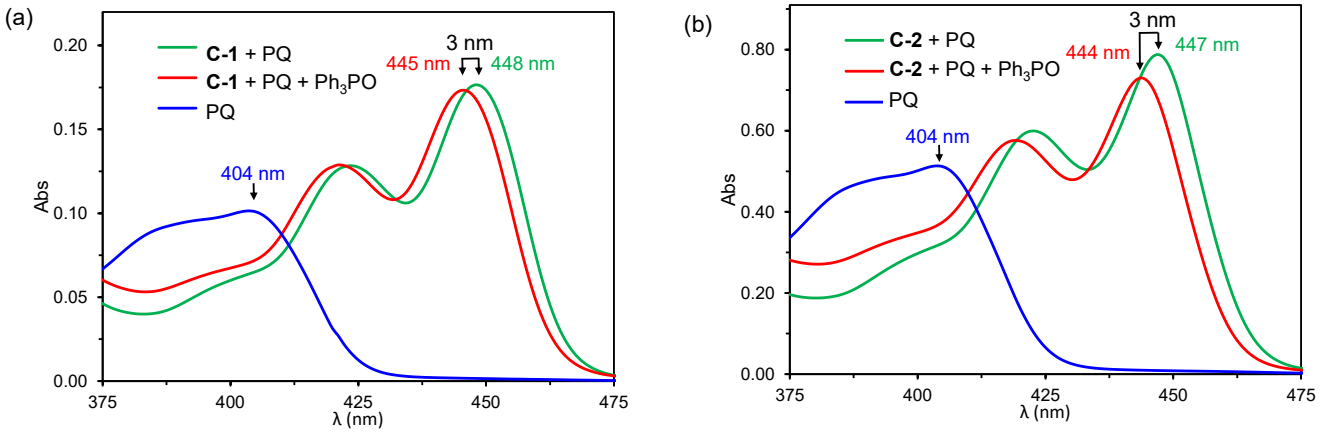

Figure S26. Comparison of the UV-Vis of the cages **C-1** and **C-2** with pentacenequinone (PQ) in CH_2Cl_2 at room temperature: (a) 20 μM **C-1**, 10 μM PQ, and 1 mM Ph_3PO; (b) 100 μM **C-1**, 50 μM PQ, and 5 mM Ph_3PO.

Determination of Diels–Alder reaction kinetic parameters

Experimental details

The kinetic experiments were monitored by ^{1}H NMR using the following procedure: To an NMR tube was introduced a stock solution containing the cage (**C-1** or **C-2**) compound (450 μL of a stock solution 0.56 mM in CD_2Cl_2) or just CD_2Cl_2 (450 μL) for the uncatalyzed reactions, quinone (20 μL of a stock solution 62.5 mM in CD_2Cl_2), and the internal standard tetrakis(trimethylsilyl)silane (10 μL of a stock solution 15.2 mM in CD_2Cl_2). The Diels–Alder reaction was then started by the addition of the corresponding diene (20 μL of a stock solution in CD_2Cl_2, 5–10 equivalents depending on diene reactivity). ^{1}H NMR spectra were recorded at regular intervals until sufficient data was collected to determine the kinetic parameters. In all cases the NMR reactions were kept at 298 K. Kinetic ^{1}H NMR data was processed using the MestreNova 11 software and the concentration of all chemical species were determined for each reaction time. All reactions were performed at least twice and a representative example is reported in the supporting information.

Experimental kinetic constants for the catalyzed reaction (k_{cat}) were obtained by fitting to the simulated kinetic model using the Levenberg-Marquardt Nonlinear Least-Squares Algorithm[S3] implemented in the R software[S4] and the RStudio[S5] software interface. Fittings were carried out simultaneously to the formation of the product and disappearance of the quinone minimizing the fitting mathematical errors and ensuring that the data fits to the kinetic model. The determined concentration by ^{1}H NMR spectroscopy corresponds to the total concentration of quinone and Diels–Alder adduct as long they are in fast exchange with the supramolecular complexes of the different catalyst species described in Figure S27. Therefore the fittings were performed to A+E+J+K (total quinone concentration, free and bound to the catalyst) and C+F+L+M (total Diels–Alder adduct concentration, free and bound to the catalyst). The association constants of the quinones were determined by ^{1}H NMR titrations and the association constants of the Diels–Alder adducts ($K_{P\,Ass}$) were determined either by ^{1}H NMR titrations or estimated form the kinetic experiments (in this last case, the changes in the chemical shifts of the cage, quinone and Diels–Alder adduct were additionally used to identify whether the Diels–Alder adducts bound stronger or weaker than the substrate). The observed kinetic constant (k_{Obs}) was obtained by fitting the data to the uncatalyzed reaction model (A + B → C).

Kinetic models

The kinetic model considers both the second order uncatalyzed background and the second order catalyzed reactions (steps 3, 11 and 13 in Figure S27) by the cage compound. The active species E, J and M are obtained by the formation of a supramolecular complex between the quinone and the cage compound (steps 2, 7, 8, 9 and 10 in Figure S27). The model also considers the possible product inhibition by the formation of a supramolecular complex between the Diels–Alder adduct and the cage compound (steps 4, 12 and 14 in Figure S27). All the equilibria steps are assumed to be fast relative to cycloaddition, in accordance with NMR observations. From the reactions described in Figure S27 the corresponding set of differential equations were solved using the package *deSolve*[S10] implemented in the R software[S4] and the RStudio[S5] software interface.

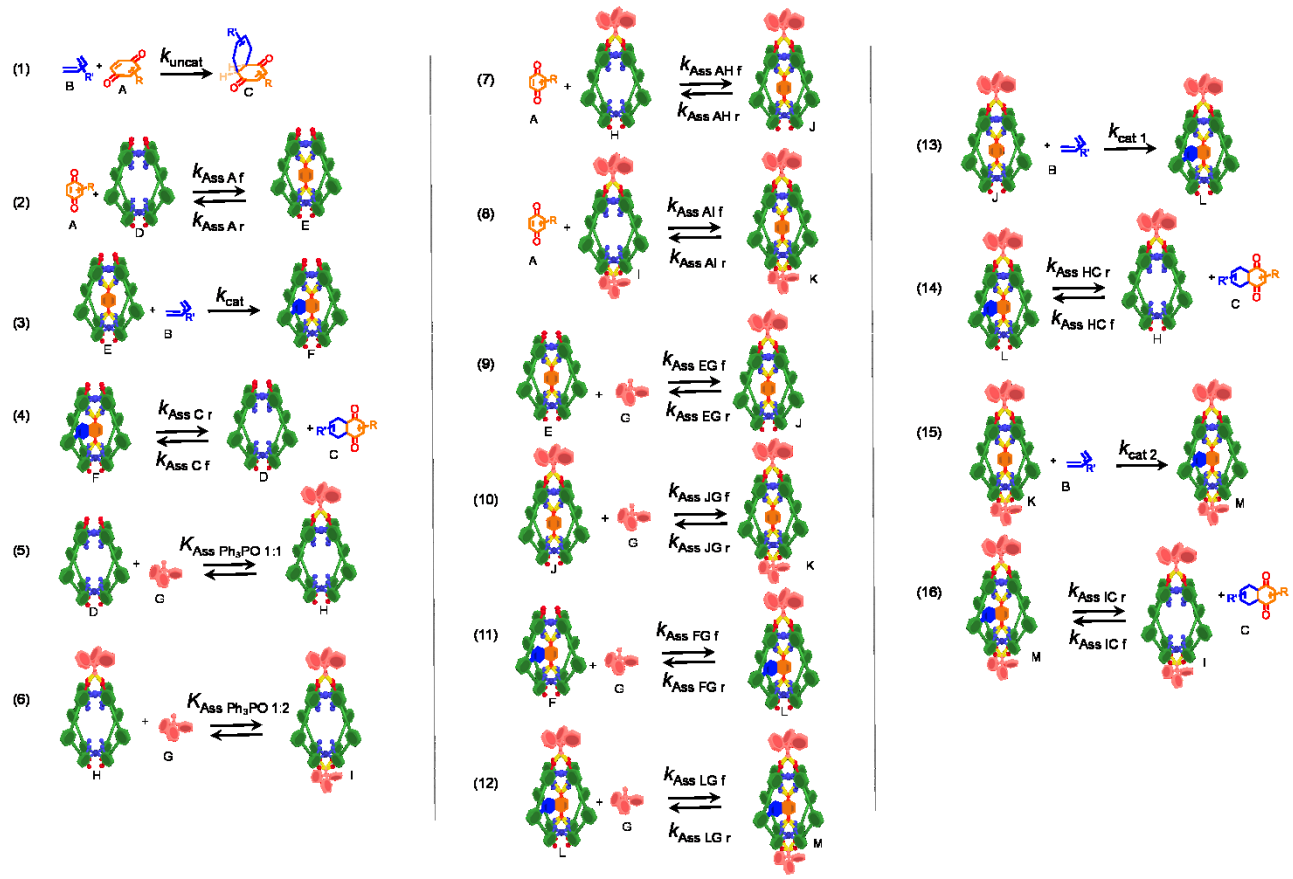

Figure S27. Cage catalyzed Diels–Alder reaction mechanism in the presence of Ph_3PO.

$d[A]/dt = - k_{uncat}\cdot[A]\cdot[B] - k_{assAf}\cdot[A]\cdot[D] + k_{assAr}\cdot[E] - k_{assAHf}\cdot[H]\cdot[A] + k_{assAHr}\cdot[J] - k_{assAIf}\cdot[I]\cdot[A] + k_{assAIr}\cdot[K]$

$d[B]/dt = - k_{uncat}\cdot[A]\cdot[B] - k_{cat}\cdot[E]\cdot[B] - k_{cat1}\cdot[J]\cdot[B] - k_{cat2}\cdot[K]\cdot[B]$

$d[C]/dt = + k_{uncat}\cdot[A]\cdot[B] + k_{assCr}\cdot[F] - k_{assCf}\cdot[D]\cdot[C] + k_{assHCr}\cdot[L] - k_{assHCf}\cdot[H]\cdot[C] + k_{assICr}\cdot[M] - k_{assICf}\cdot[I]\cdot[C]$

$d[D]/dt = - k_{assAf}\cdot[A]\cdot[D] + k_{assAr}\cdot[E] + k_{assCr}\cdot[F] - k_{assCf}\cdot[D]\cdot[C] - k_{assDGf}\cdot[D]\cdot[G] + k_{assDGr}\cdot[H]$

$d[E]/dt = + k_{assAf}\cdot[A]\cdot[D] - k_{assAr}\cdot[E] - k_{cat}\cdot[E]\cdot[B] - k_{assEGf}\cdot[E]\cdot[G] + k_{assEGr}\cdot[J]$

$d[F]/dt = + k_{cat}\cdot[E]\cdot[B] - k_{assCr}\cdot[F] + k_{assCf}\cdot[D]\cdot[C] - k_{assFGf}\cdot[F]\cdot[G] + k_{assFGr}\cdot[L]$

$d[G]/dt = - k_{assDGf}\cdot[D]\cdot[G] + k_{assDGr}\cdot[H] - k_{assHGf}\cdot[H]\cdot[G] + k_{assHGr}\cdot[I] - k_{assEGf}\cdot[E]\cdot[G] + k_{assEGr}\cdot[J] - k_{assJGf}\cdot[J]\cdot[G] + k_{assJGr}\cdot[K] - k_{assFGf}\cdot[F]\cdot[G] + k_{assFGr}\cdot[L] - k_{assLGf}\cdot[L]\cdot[G] + k_{assLGr}\cdot[M]$

$d[H]/dt = + k_{assDGf}\cdot[D]\cdot[G] - k_{assDGr}\cdot[H] - k_{assHGf}\cdot[H]\cdot[G] + k_{assHGr}\cdot[I] - k_{assAHf}\cdot[H]\cdot[A] + k_{assAHr}\cdot[J] + k_{assHCr}\cdot[L] - k_{assHCf}\cdot[H]\cdot[C]$

$d[I]/dt = + k_{assHGf}\cdot[H]\cdot[G] - k_{assHGr}\cdot[I] - k_{assAIf}\cdot[I]\cdot[A] + k_{assAIr}\cdot[K] + k_{assICr}\cdot[M] - k_{assICf}\cdot[I]\cdot[C]$

$d[J]/dt = + k_{assAHf}\cdot[H]\cdot[A] - k_{assAHr}\cdot[J] + k_{assEGf}\cdot[E]\cdot[G] - k_{assEGr}\cdot[J] - k_{assJGf}\cdot[J]\cdot[G] + k_{assJGr}\cdot[K] - k_{cat1}\cdot[J]\cdot[B]$

$d[K]/dt = + k_{assAIf}\cdot[I]\cdot[A] - k_{assAIr}\cdot[K] + k_{assJGf}\cdot[J]\cdot[G] - k_{assJGr}\cdot[K] - k_{cat2}\cdot[K]\cdot[B]$

$d[L]/dt = + k_{cat1}\cdot[J]\cdot[B] - k_{assHCr}\cdot[L] + k_{assHCf}\cdot[H]\cdot[C] + k_{assFGf}\cdot[F]\cdot[G] - k_{assFGr}\cdot[L] - k_{assLGf}\cdot[L]\cdot[G] + k_{assLGr}\cdot[M]$

$d[M]/dt = + k_{cat2}\cdot[K]\cdot[\text{"B"}] - k_{assMr}\cdot[M] + k_{assMf}\cdot[I]\cdot[C] + k_{assLGf}\cdot[L]\cdot[G] - k_{assLGr}\cdot[M]$

The kinetic constant and association constants for species involving one Ph_3PO were estimated assuming that $\Delta G_{cage\cdot(Ph_3PO)} = 1/2\times(\Delta G_{cage} + \Delta G_{cage\cdot(Ph_3PO)_2})$ using the following equations:[S11]

$k_{cat1} = (k_{cat} \times k_{cat2})^{1/2}$

$K_{assHA} = (K_{assA} \times K_{assIA})^{1/2}$

$K_{assHC} = (K_{assC} \times K_{assIC})^{1/2}$

Kinetic data for individual DA reactions

Reaction of benzoquinone and isoprene

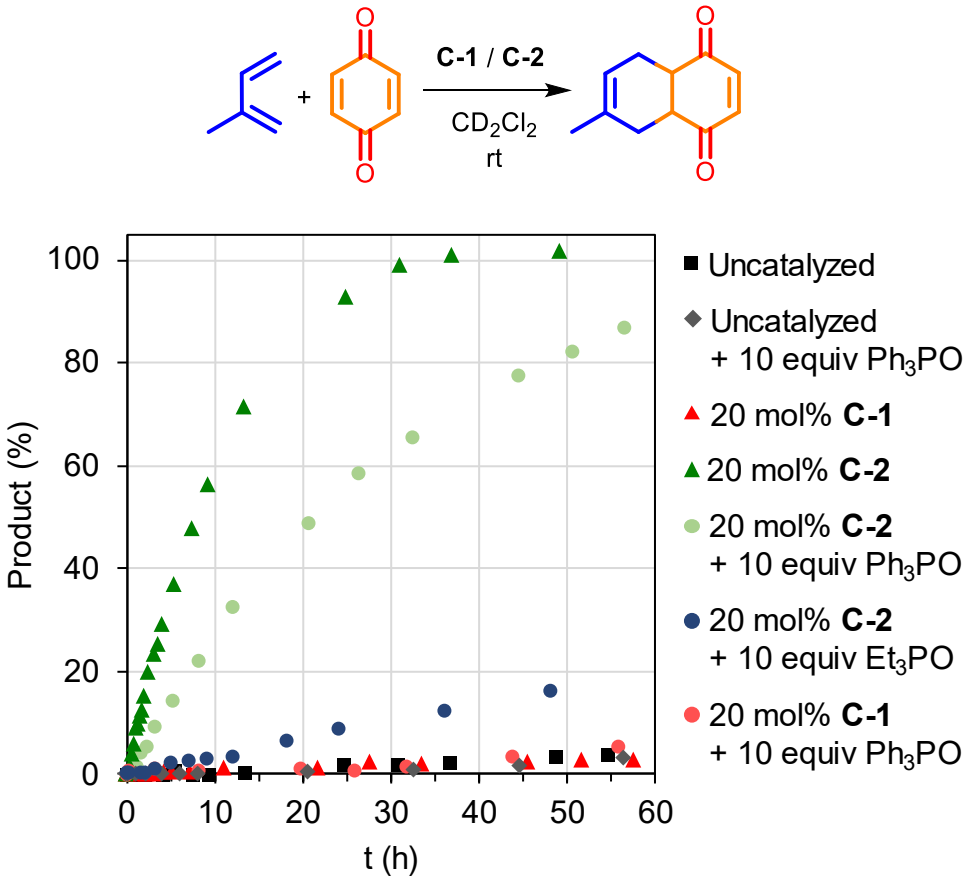

Figure S28. Diels–Alder kinetic data for the reaction of benzoquinone with isoprene. Cage **C-2** gives significant acceleration (green triangles) and structurally similar **C-1** (red triangles) gives no enhancement compared to the uncatalyzed reaction (black squares). Addition of Ph_3PO to cage **C-2** (pale green circles) maintains the catalytic activity. Addition of Et_3PO to cage **C-2** (dark blue circles) significantly reduces the catalytic activity. Addition of Ph_3PO to cage **C-1** (pale red circles) does produce any effect. Addition of Ph_3PO to uncatalyzed reaction does not produce any effect (grey diamonds). Data for the background reaction, **C-1** and **C-2** catalyzed reactions from ref [S2].

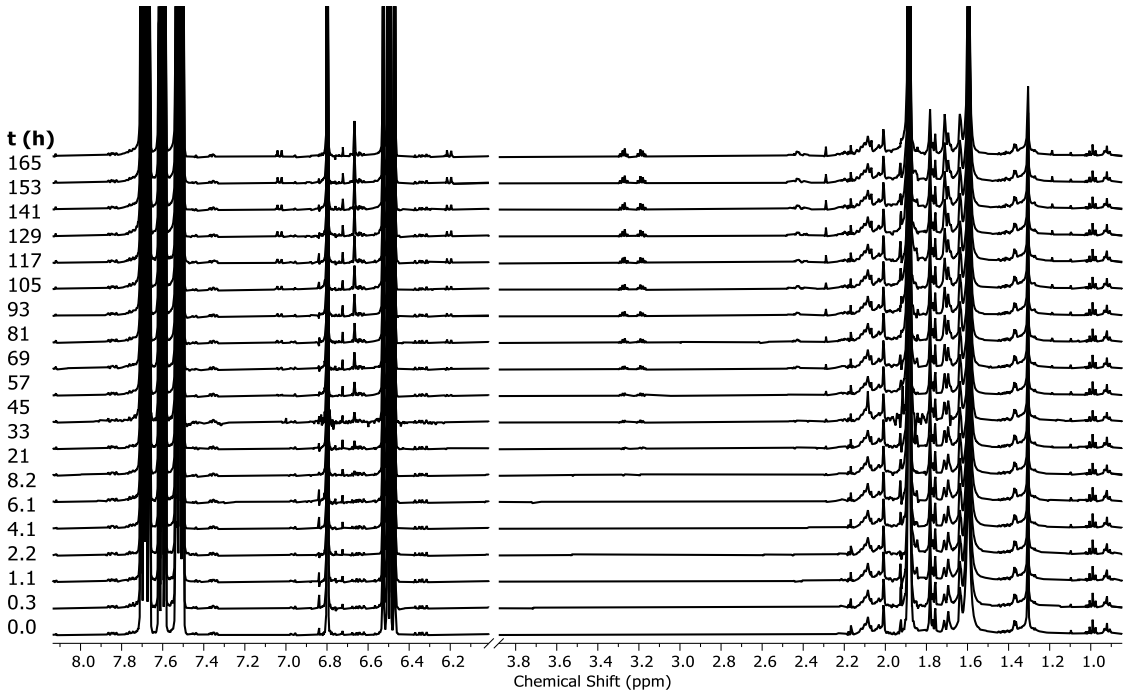

Figure S29. ^{1}H NMR spectra (500 MHz, CD_2Cl_2) for the reaction of benzoquinone (2.5 mM) and isoprene (25 mM) in the presence of Ph_3PO (5 mM).

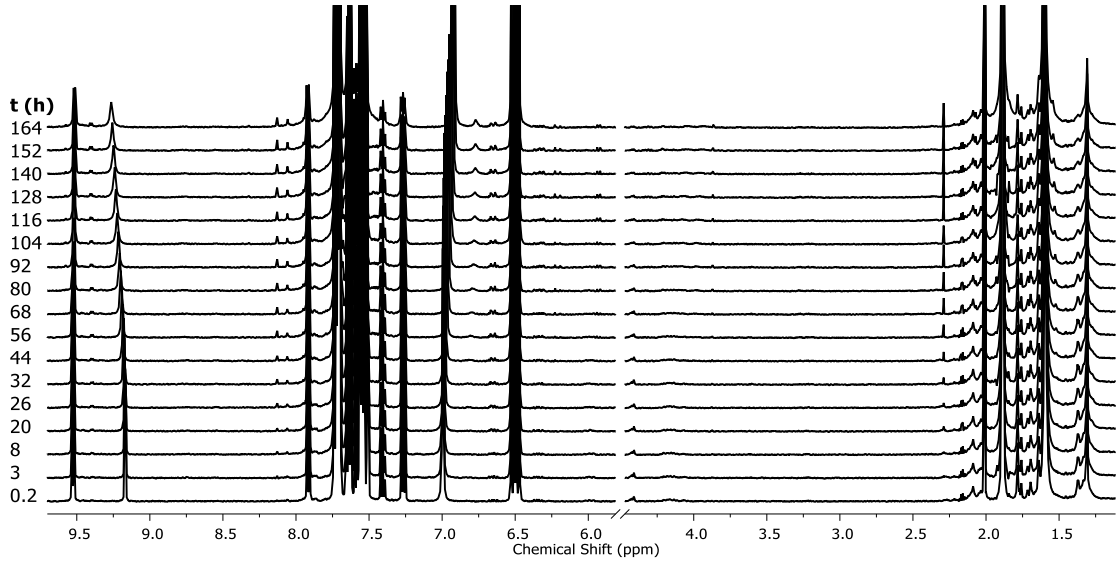

Figure S30. ^{1}H NMR spectra (500 MHz, CD_2Cl_2) for the reaction of benzoquinone (2.5 mM) and isoprene (25 mM) in the presence of the cage **C-1** (0.45 mM) and Ph_3PO (5 mM).

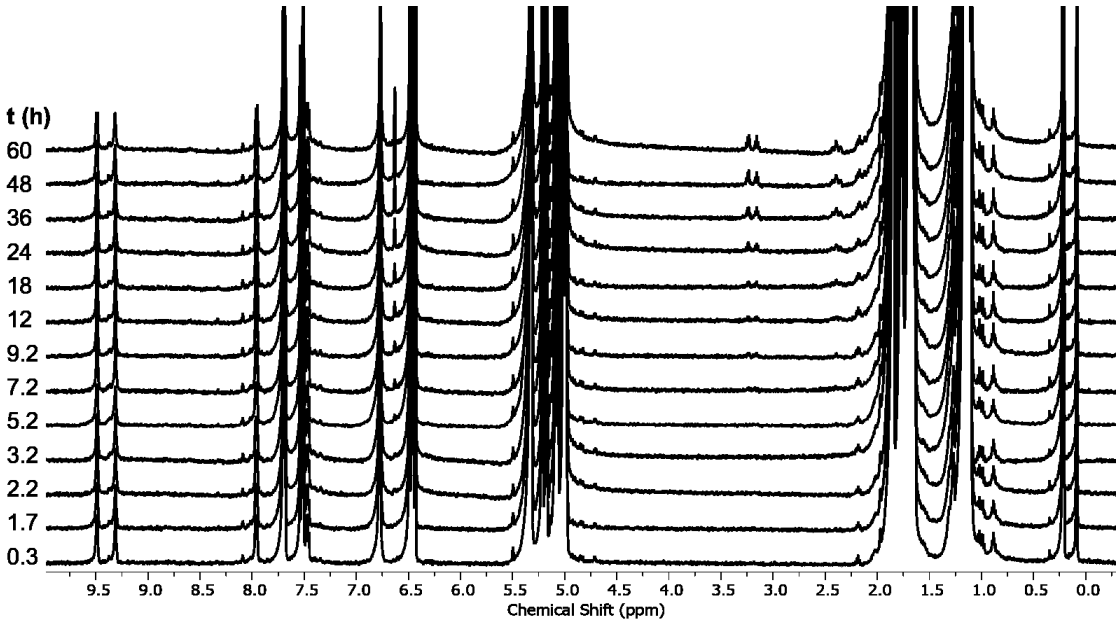

Figure S31. ^{1}H NMR spectra (500 MHz, CD_2Cl_2) for the reaction of benzoquinone (2.5 mM) and isoprene (25 mM) in the presence of the cage **C-2** (0.5 mM) and Et_3PO (5 mM).

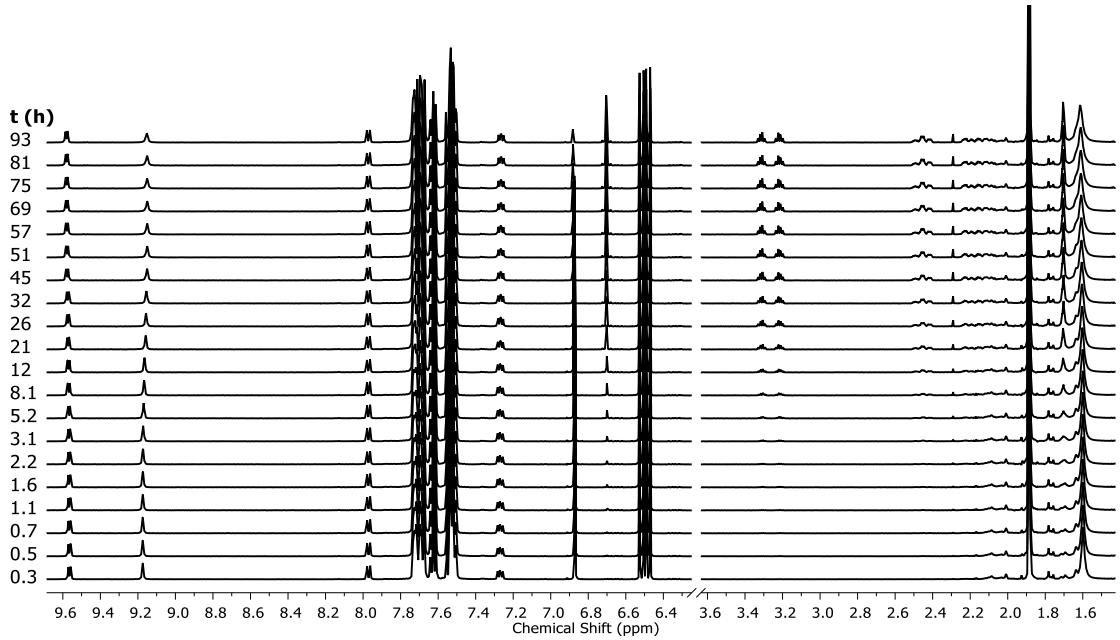

Figure S32. ^{1}H NMR spectra (500 MHz, CD_2Cl_2) for the reaction of benzoquinone (2.5 mM) and isoprene (25 mM) in the presence of the cage **C-2** (0.45 mM) and Ph_3PO (5 mM).

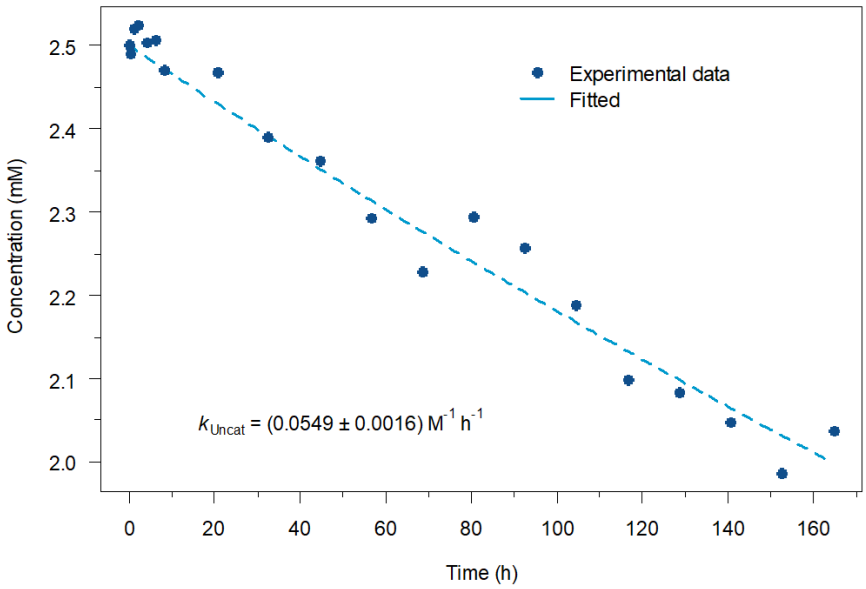

Figure S33. Kinetic fitting for the uncatalyzed reaction of benzoquinone and isoprene.

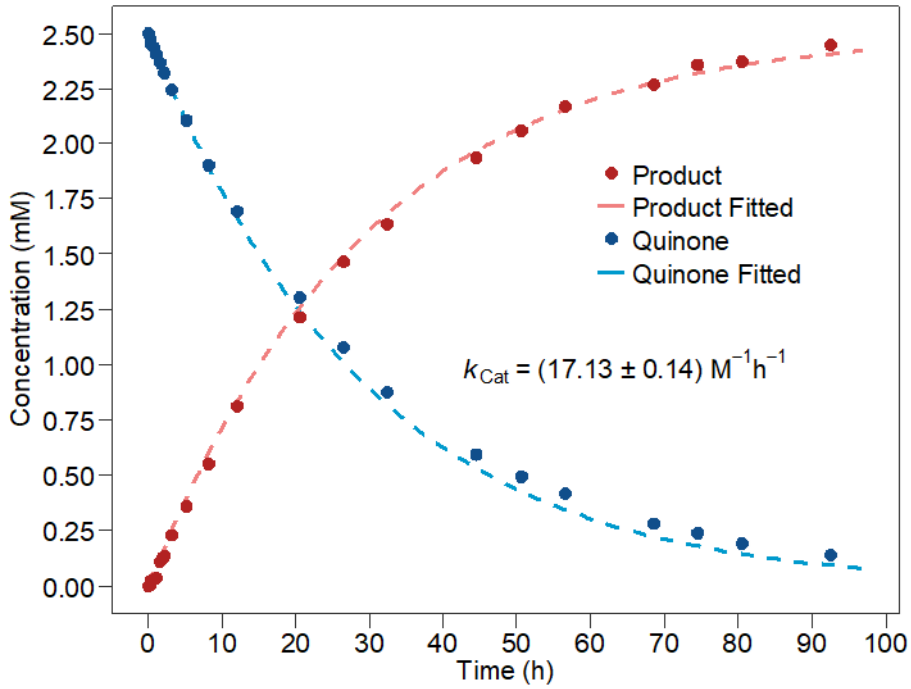

Figure S34. Kinetic fitting for the catalyzed reaction of benzoquinone and isoprene in the presence of the cage **C-2** and Ph_3PO. Using $K_{Ass\ \mathbf{C\text{-}2}\ Product}$ = 510 M^{-1} and k_{cat} = 23.6 M^{-1} h^{-1}, k_{uncat} = 0.060 M^{-1} h^{-1} from ref [S2]; $K_{ass\ \mathbf{C\text{-}2}\ Ph_3PO\ 1:1}$ = 8200 M^{-1}, $K_{ass\ \mathbf{C\text{-}2}\ Ph_3PO\ 1:2}$= 2100 M^{-1}, $K_{ass\ [Benzoquinone\subset\mathbf{C\text{-}2}]\ Ph_3PO\ 1:1}$ = 4300 M^{-1}, $K_{ass\ [Benzoquinone\subset\mathbf{C\text{-}2}]\ Ph_3PO\ 1:2}$= 1100 M^{-1}, and estimating $K_{ass\ [Product\subset\mathbf{C\text{-}2}]\ Ph_3PO\ 1:1}$ = 4300 M^{-1}, $K_{ass\ [Product\subset\mathbf{C\text{-}2}]\ Ph_3PO\ 1:2}$= 1100 M^{-1}, $K_{Ass\ \mathbf{C\text{-}2}\cdot(Ph_3PO)_2\text{-}Product}$ = 116 M^{-1}.

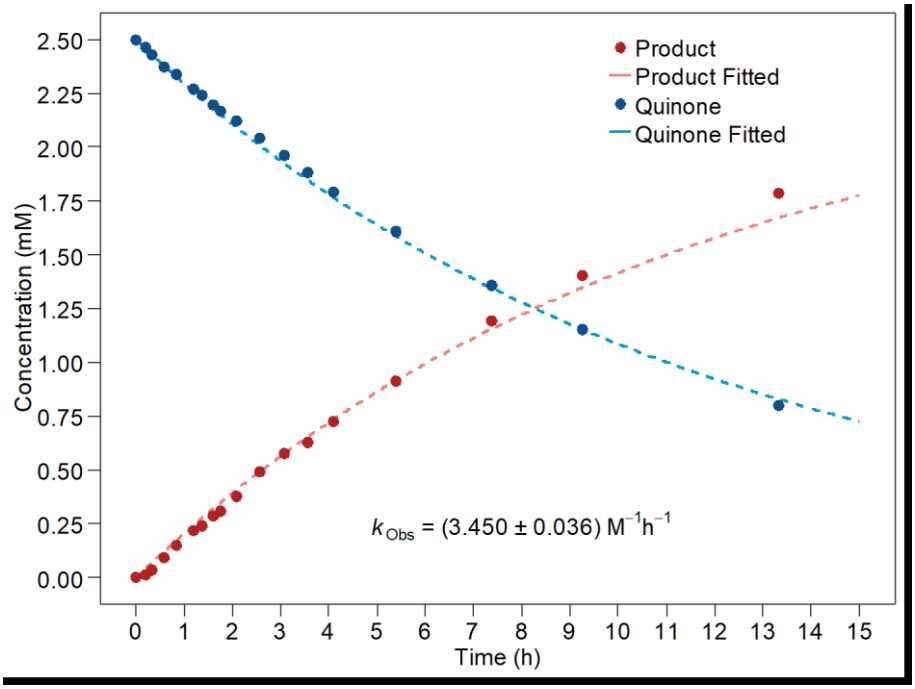

Figure S35. Kinetic fitting to obtain k_{Obs} for the catalyzed reaction of benzoquinone and isoprene in the presence of the cage **C-2**. Data from ref [S2].

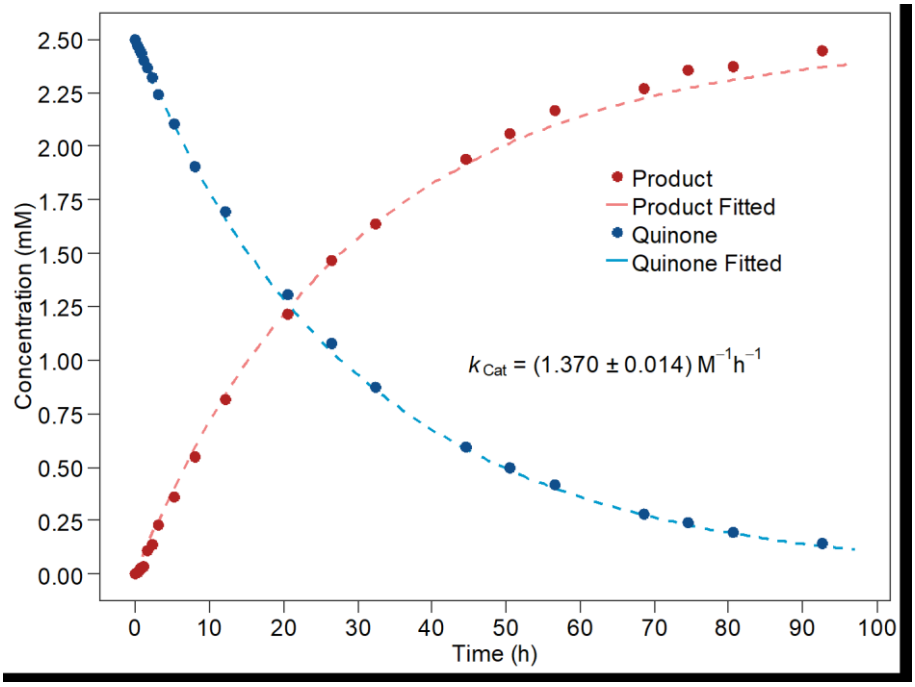

Figure S36. Kinetic fitting to obtain k_{Obs} for the catalyzed reaction of benzoquinone and isoprene in the presence of the cage **C-2** and Ph_3PO.

Reaction of benzoquinone and cyclohexadiene

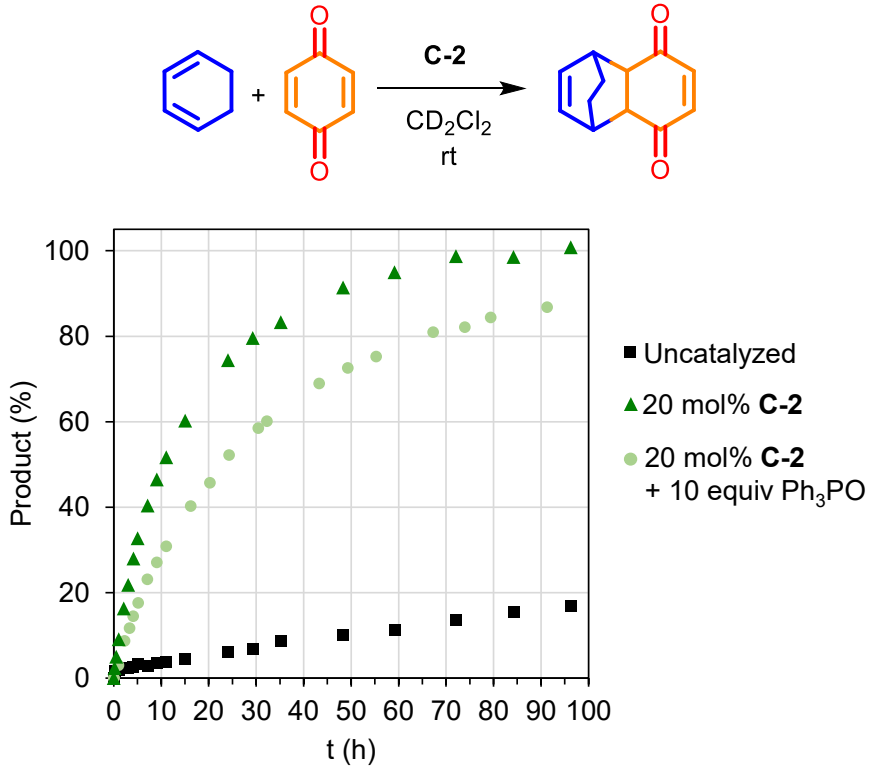

Figure S37. Diels–Alder kinetic data for the reaction of benzoquinone with cyclohexadiene. Cage **C-2** gives significant acceleration (green triangles) will little evidence of product inhibition. Addition of Ph_3PO to cage **C-2** (pale green circles) maintains the catalytic activity. Data for the background reaction and **C-2** catalyzed reactions from ref [S2].

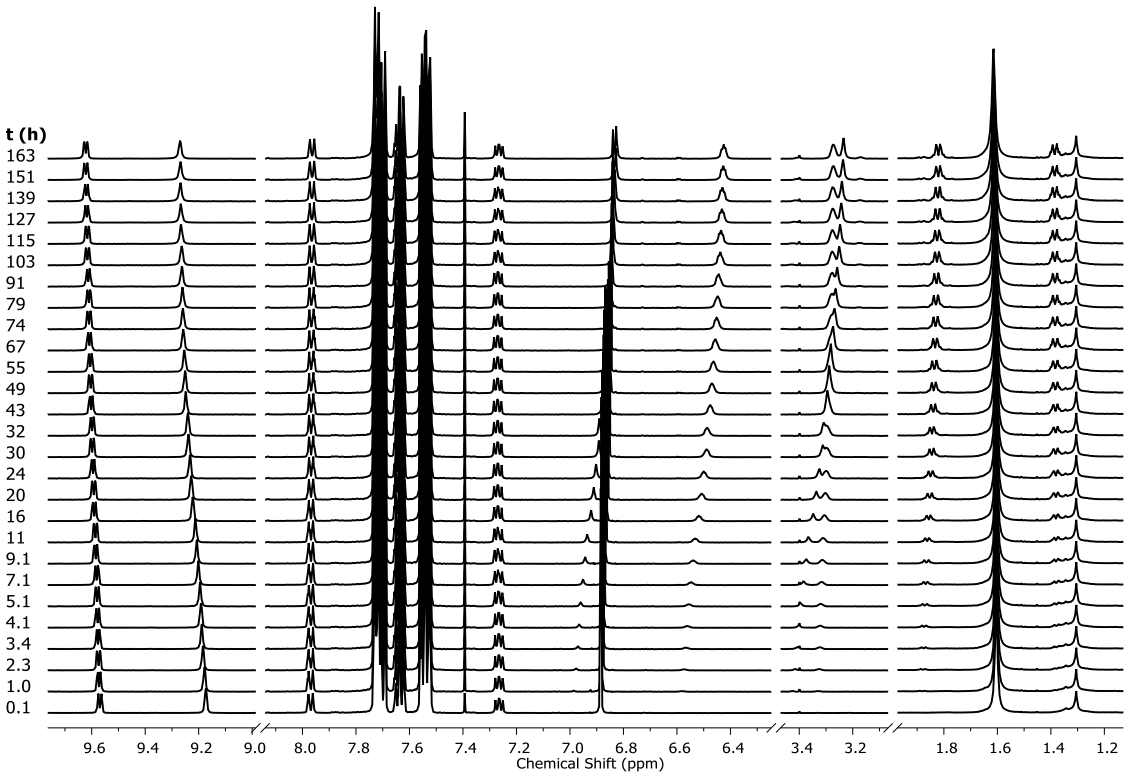

Figure S38. ^{1}H NMR spectra (500 MHz, CD_2Cl_2) for the reaction of benzoquinone (2.5 mM) and cyclohexadiene (12.5 mM) in the presence of the cage **C-2** (0.50 mM) and $OPPh_3$ (5 mM).

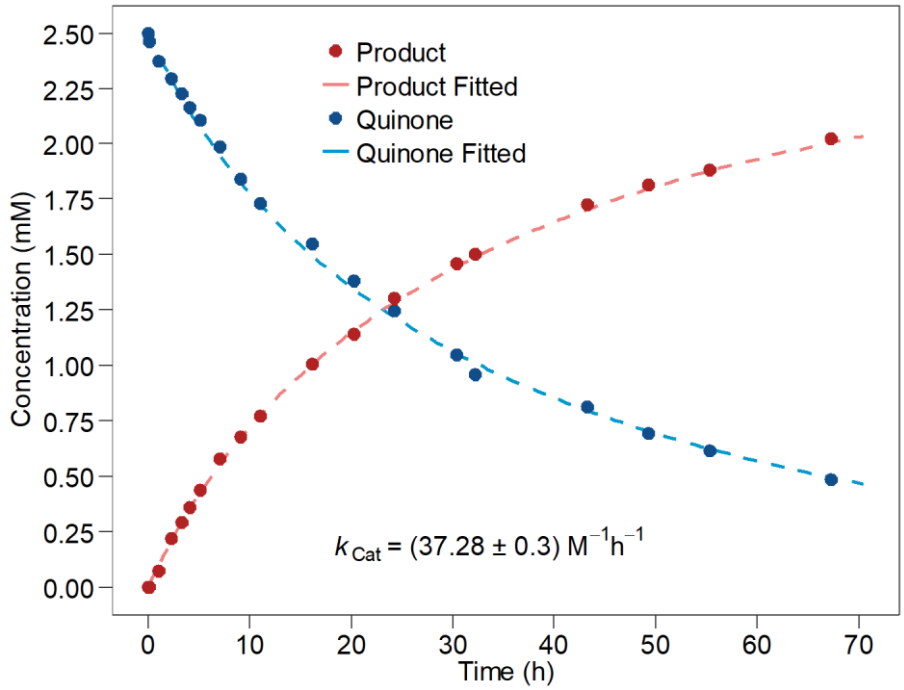

Figure S39. Kinetic fitting for the catalyzed reaction of benzoquinone and cyclohexadiene in the presence of the cage **C-2** and Ph_3PO. Using $K_{Ass\ \mathbf{C\text{-}2}\ Product}$ = 4600 M^{-1}, k_{cat} = 61 M^{-1} h^{-1}, k_{uncat} = 0.20 M^{-1} h^{-1}, from ref [S2]; $K_{ass\ \mathbf{C\text{-}2}\ Ph_3PO\ 1:1}$ = 8200 M^{-1}, $K_{ass\ \mathbf{C\text{-}2}\ Ph_3PO\ 1:2}$= 2100 M^{-1}, $K_{ass\ [Benzoquinone\subset\mathbf{C\text{-}2}]\ Ph_3PO\ 1:1}$ = 4300 M^{-1}, $K_{ass\ [Benzoquinone\subset\mathbf{C\text{-}2}]\ Ph_3PO\ 1:2}$= 1100 M^{-1}, estimating $K_{ass\ [Product\subset\mathbf{C\text{-}2}]\ Ph_3PO\ 1:1}$ = 4300 M^{-1}, $K_{ass\ [Product\subset\mathbf{C\text{-}2}]\ Ph_3PO\ 1:2}$= 1100 M^{-1}, and obtaning from the fitting $K_{Ass\ \mathbf{C\text{-}2}(Ph_3PO)_2\text{-}Product}$ = (880 ± 70) M^{-1}.

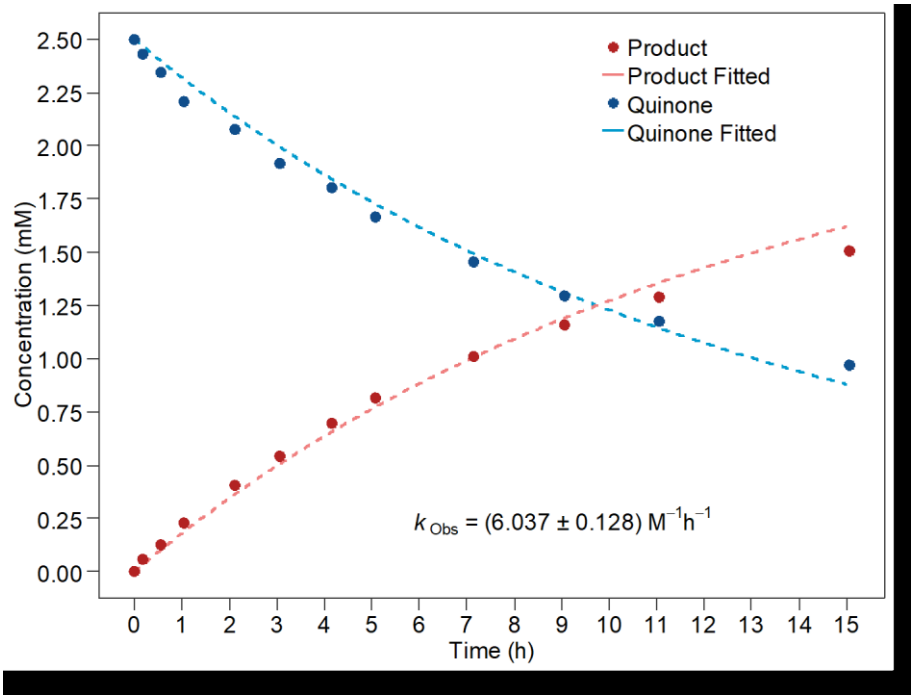

Figure S40. Kinetic fitting to obtain k_{Obs} for the catalyzed reaction of benzoquinone and cyclohexadiene in the presence of the cage **C-2**. Data from ref [S2].

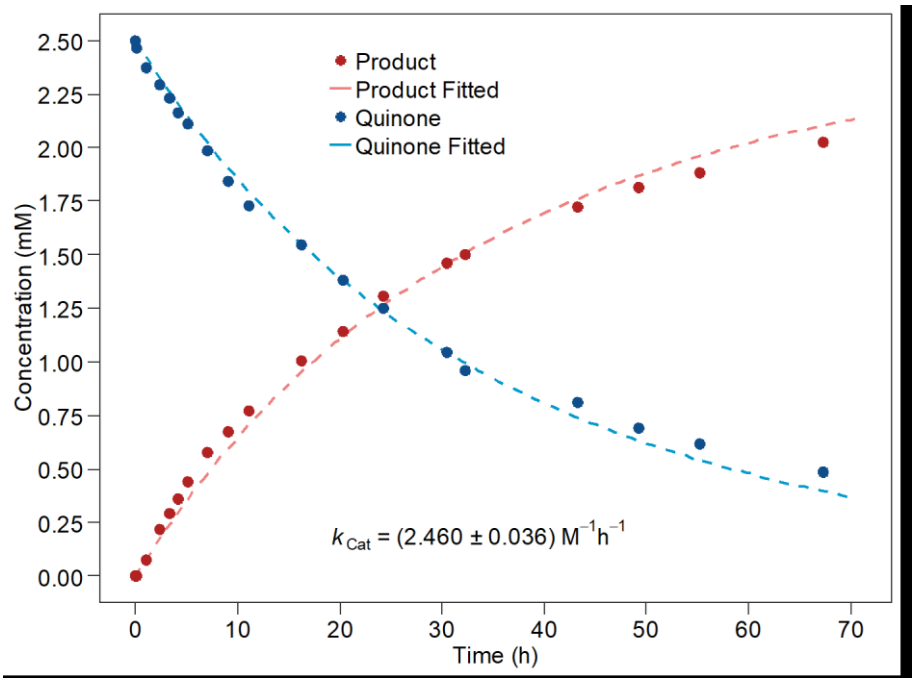

Figure S41. Kinetic fitting to obtain k_{Obs} for the catalyzed reaction of benzoquinone and cyclohexadiene in the presence of the cage **C-2** and Ph_3PO.

X ray crystallography

Crystal structure of [pentacenequinone⊂**C-1**]·$(OTf)_4$,[S1] **C-1**·$(OTf)_4$,[S12] **C-2**·$(SbF_6)_4$,[S13] **C-2**·$(OMs)_4$,[S14] **C-2**·$(OTf)_4$,[S14] and **C-2**·$(BF_4)_4$[S15] were obtained from the literature. The crystal structure of [pentacenequinone⊂**C-2**]·$(BArF)_4$ is described below.

Overlay of cages crystal structures

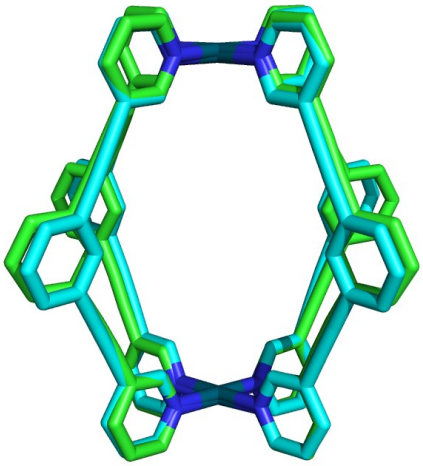

Figure S42. Overlay of the crystal structures of [pentacenequinone⊂**C-1**]·$(OTf)_4$ (green), **C-1**·$(OTf)_4$ (cyan).

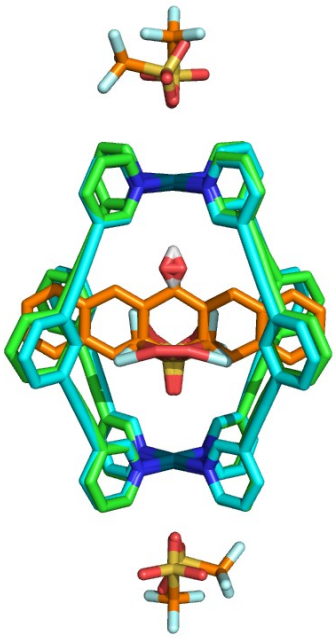

Figure S43. Overlay of the crystal structures of [pentacenequinone⊂**C-1**]·$(OTf)_4$ (green), **C-1**·$(OTf)_4$ (cyan) showing the counteranions and solvent molecules in short distance/hydrogen bonding with the cage polarized CH protons. BArF counter anions have not been represented for clarity.

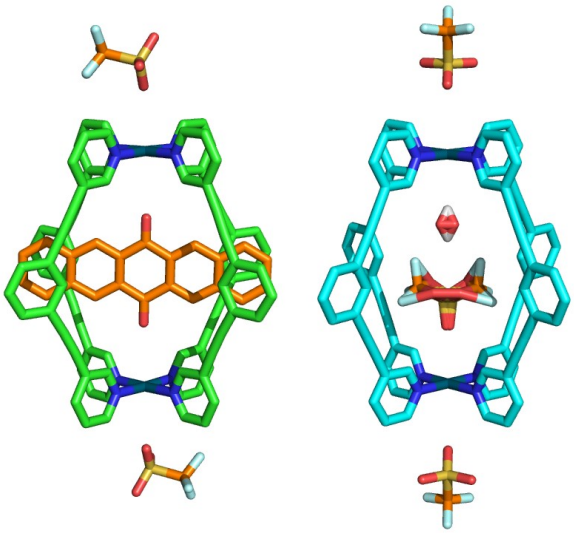

Figure S44. Comparison of the crystal structures of [pentacenequinone⊂**C-1**]·$(OTf)_4$ (green), **C-1**·$(OTf)_4$ (cyan) showing the counteranions and solvent molecules in short distance/hydrogen bonding with the cage polarized CH protons. BArF counter anions have not been represented for clarity.

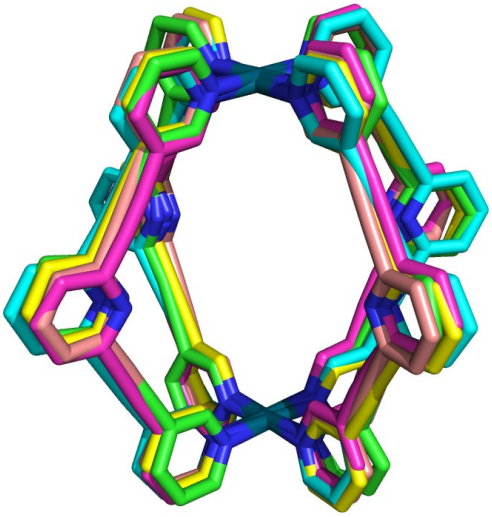

Figure S45. Overlay of the crystal structures of [pentacenequinone⊂**C-2**]·$(BArF)_4$ (green), **C-2**·$(SbF_6)_4$ (cyan), **C-2**·$(OMs)_4$ (purple), **C-2**·$(OTf)_4$ (yellow), **C-2**·$(BF_4)_4$ (pale red).

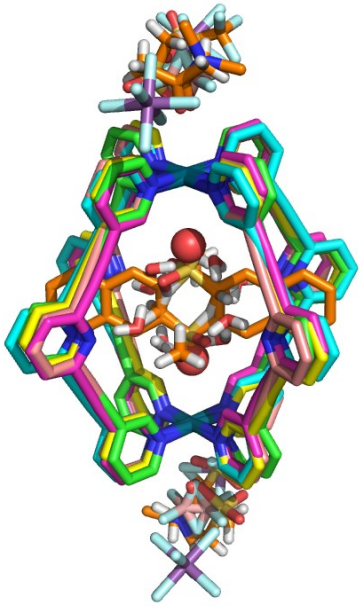

Figure S46. Overlay of the crystal structures of [pentacenequinone⊂**C-2**]·$(BArF)_4$ (green), **C-2**·$(SbF_6)_4$ (cyan), **C-2**·$(OMs)_4$ (purple), **C-2**·4$(OTf)_4$ (yellow), **C-2**·$(BF_4)_4$ (pale red) showing the counteranions and solvent molecules in short distance/hydrogen bonding with the cage polarized CH protons. BArF counter anions have not been represented for clarity.

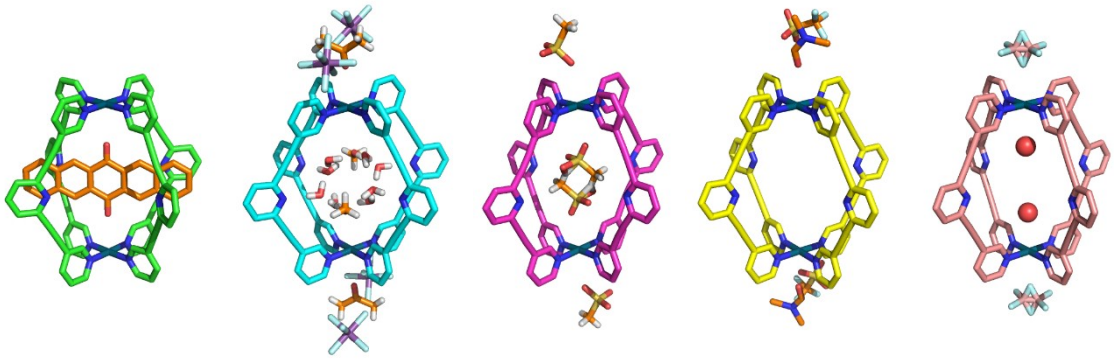

Figure S47. Crystal structures of [pentacenequinone⊂**C-2**]·$(BArF)_4$ (green), **C-2**·$(SbF_6)_4$ (cyan), **C-2**·4$(OMs)_4$ (purple), **C-2**·$(OTf)_4$ (yellow), **C-2**·$(BF_4)_4$ (pale red) showing the counteranions and solvent molecules in short distance/hydrogen bonding with the cage polarized CH protons. BArF counter anions have not been represented for clarity.

Crystal data of [pentacenequinone⊂C-2]·$(BArF)_4$

Single crystals of pentacenequinone⊂**C-1** were obtained by vapour diffusion of diisopropyl ether to a solution of **1** in CH_2Cl_2. Suitable crystals were selected and for single-crystal using a SuperNova, Dual, Cu at zero, Atlas diffractometer. The crystal was kept at 120.00(10) K during data collection. Disordered solvent (not reported in the calculated formula) could not be modelled and it's corresponding electron density was removed using the SQUEEZE routine of PLATON.[S16] Using Olex2,[S17] the structure was solved with the ShelXT[S18] structure solution program using Direct Methods and refined with the ShelXL[S19] refinement package using Least Squares minimisation. All non-hydrogen atoms were refined with anisotropically, and all hydrogen atoms were added and refined isotropically using a riding model.

Crystal data for [pentacenequinone⊂**C-2**]·(BArF)$_4$ ($C_{228}H_{104}B_4Cl_4F_{96}N_{12}O_2Pd_2$, M =5265.07 g/mol): monoclinic, space group C2/c (no. 15), a = 40.6116(6) Å, b = 14.3027(2) Å, c = 43.1791(9) Å, β = 108.163(2)°, V = 23831.1(7) Å^3, Z = 4, T = 120.00(10) K, μ(CuKα) = 2.796 mm^{-1}, *Dcalc* = 1.467 g/cm^3, 189819 reflections measured (6.59° ≤ 2Θ ≤ 153.096°), 24792 unique (R_{int} = 0.0906, R_{sigma} = 0.0615) which were used in all calculations. The final R_1 was 0.0936 (I > 2σ(I)) and wR_2 was 0.2569 (all data).

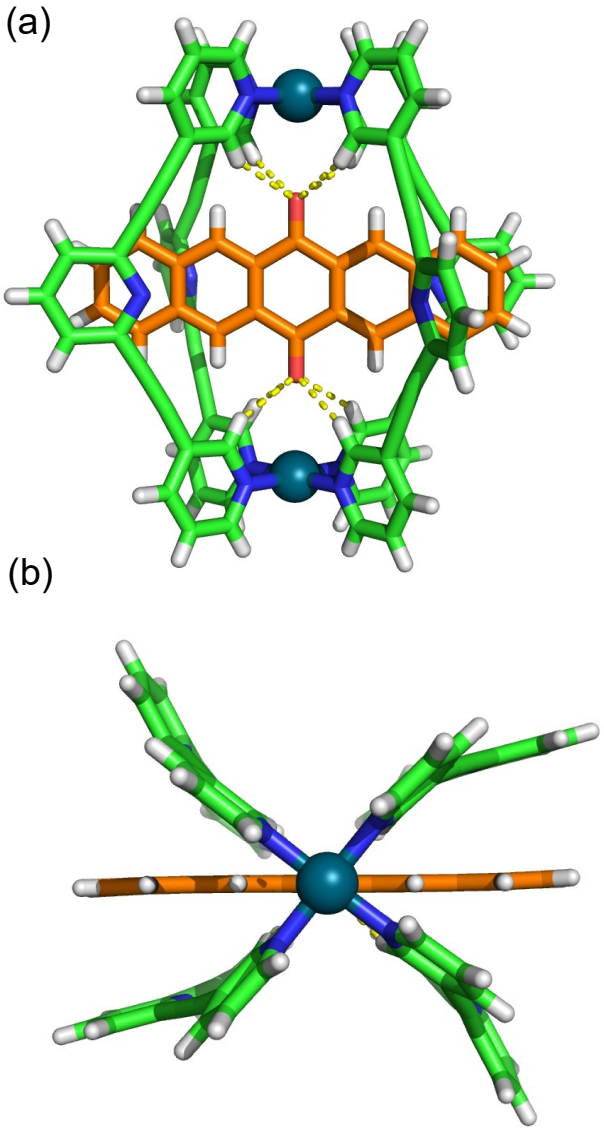

Figure S48. Crystal structure of pentacenequinone (orange) encapsulated within cage **C-2** (green). Solvent and counter ions are omitted for clarity. One of the central ligand pyridine rings of the cage is disordered in two parts, only the part with a larger occupancy has been represented for clarity. (a) Front view showing the 8 H-bonds between the pentacenequinone and the cage, (b) top view showing the bend of the ligand.

Table S1. Crystal data and structure refinement for pentacenequinone⊂**C-2**.

Empirical formula	$C_{228}H_{104}B_4Cl_4F_{96}N_{12}O_2Pd_2$
Formula weight	5265.07
Temperature/K	120.00(10)
Crystal system	monoclinic
Space group	C2/c
a/Å	40.6116(6)
b/Å	14.3027(2)
c/Å	43.1791(9)
α/°	90
β/°	108.163(2)
γ/°	90
Volume/Å^3	23831.1(7)
Z	4
ρ_{calc}g/cm^3	1.467
μ/mm^{-1}	2.796
F(000)	10464.0
Crystal size/mm^3	0.509 × 0.188 × 0.049
Radiation	CuKα (λ = 1.54178)
2Θ range for data collection/°	6.59 to 153.096
Index ranges	-48 ≤ h ≤ 50, -17 ≤ k ≤ 18, -54 ≤ l ≤ 54
Reflections collected	189819
Independent reflections	24792 [R_{int} = 0.0906, R_{sigma} = 0.0615]
Data/restraints/parameters	24792/728/1790
Goodness-of-fit on F^2	1.103
Final R indexes [I>=2σ (I)]	R_1 = 0.0936, wR_2 = 0.2486
Final R indexes [all data]	R_1 = 0.1031, wR_2 = 0.2572
Largest diff. peak/hole / e Å^{-3}	1.46/-1.20

Table S2. Bond Lengths for pentacenequinone⊂**C-2**.

Atom	Atom	Length/Å	Atom	Atom	Length/Å
Pd1	N1	2.007(4)	F31	C95	1.335(7)
Pd1	N3^1	2.014(4)	F32	C95	1.339(8)
Pd1	N4	2.015(5)	F33	C95	1.334(7)
Pd1	N6^1	2.000(5)	F34	C96	1.305(7)
N1	C1	1.350(5)	F35	C96	1.342(6)
N1	C5	1.346(6)	F36	C96	1.319(7)
N3	Pd1^1	2.014(4)	F37	C103	1.354(6)
N3	C16	1.336(6)	F38	C103	1.344(6)
N3	C17	1.337(5)	F39	C103	1.329(6)
N4	C20	1.347(7)	F40	C104	1.324(8)
N4	C24	1.358(6)	F41	C104	1.343(8)
N5	C27	1.350(7)	F42	C104	1.332(9)
N5	C31	1.346(8)	F43	C111	1.349(9)
N6	Pd1^1	2.000(5)	F44	C111	1.316(10)
N6	C35	1.358(6)	F45	C111	1.331(8)
N6	C36	1.343(7)	F46B	C112	1.366(10)
C1	C2	1.395(6)	F47B	C112	1.347(10)
C2	C3	1.397(7)	F48B	C112	1.346(9)
C2	C6	1.437(6)	C81	C82	1.395(8)
C3	C4	1.384(7)	C81	C86	1.399(7)
C4	C5	1.381(7)	C81	B2	1.642(8)
C6	C7	1.184(7)	C82	C83	1.384(8)

C7	C8A	1.440(11)	C83	C84	1.383(9)
C7	C8B	1.484(19)	C83	C87	1.505(9)
C13	C14	1.192(8)	C84	C85	1.388(9)
C13	C12A	1.421(12)	C85	C86	1.387(7)
C13	C12B	1.53(2)	C85	C88	1.508(8)
C14	C15	1.430(7)	C89	C90	1.404(8)
C15	C16	1.390(7)	C89	C94	1.401(8)
C15	C19	1.406(6)	C89	B2	1.643(8)
C17	C18	1.378(7)	C90	C91	1.400(8)
C18	C19	1.374(7)	C91	C92	1.381(7)
C20	C21	1.384(8)	C91	C95	1.500(8)
C21	C22	1.398(8)	C92	C93	1.386(8)
C21	C25	1.435(8)	C93	C94	1.379(8)
C22	C23	1.362(10)	C93	C96	1.495(8)
C23	C24	1.394(9)	C97	C98	1.395(7)
C25	C26	1.190(9)	C97	C102	1.410(7)
C26	C27	1.432(9)	C97	B2	1.635(8)
C27	C28	1.394(8)	C98	C99	1.391(7)
C28	C29	1.376(11)	C99	C100	1.395(7)
C29	C30	1.395(11)	C99	C103	1.493(7)
C30	C31	1.391(10)	C100	C101	1.403(8)
C31	C32	1.447(8)	C101	C102	1.377(8)
C32	C33	1.177(9)	C101	C104	1.515(8)
C33	C34	1.454(8)	C105	C106	1.401(7)
C34	C35	1.373(8)	C105	C110	1.400(8)
C34	C38	1.401(9)	C105	B2	1.636(7)
C36	C37	1.365(10)	C106	C107	1.413(8)
C37	C38	1.380(10)	C107	C108	1.384(10)
Cl1	C113	1.755(12)	C107	C111	1.487(9)
Cl2	C113	1.784(12)	C108	C109	1.386(10)
F1	C56	1.31(2)	C109	C110	1.396(8)
F2	C56	1.276(17)	C109	C112	1.507(10)
F3	C56	1.342(17)	C112	F46A	1.342(9)
F4	C57	1.352(13)	C112	F47A	1.341(9)
F5	C57	1.317(9)	C112	F48A	1.365(9)
F6	C57	1.344(11)	O1	C39	1.241(6)
F7	C64	1.391(8)	C39	C40	1.478(6)
F8	C64	1.296(7)	C39	C41[1]	1.483(7)
F9	C64	1.288(7)	C40	C41	1.430(6)
F10	C65	1.267(11)	C40	C45	1.364(7)
F11	C65	1.417(13)	C41	C39[1]	1.483(7)
F12	C65	1.300(9)	C41	C42	1.374(6)
C50	C51	1.389(9)	C42	C43	1.412(7)
C50	C55	1.403(10)	C43	C44	1.418(6)
C50	B1	1.637(10)	C43	C49	1.418(7)
C51	C52	1.375(12)	C44	C45	1.411(6)
C52	C53	1.389(14)	C44	C46	1.415(7)
C52	C56	1.500(14)	C46	C47	1.370(8)
C53	C54	1.387(12)	C47	C48	1.392(9)
C54	C55	1.368(10)	C48	C49	1.368(9)
C54	C57	1.499(13)	N0AA	C8B	1.54(3)
C58	C59	1.385(9)	N0AA	C12B	1.26(4)
C58	C63	1.381(8)	N2A	C8A	1.35(2)
C58	B1	1.648(9)	N2A	C12A	1.39(2)
C59	C60	1.393(9)	C8A	C9A	1.393(8)
C60	C61	1.375(9)	C8B	C9B	1.388(10)
C60	C64	1.454(10)	C9A	C10A	1.393(9)
C61	C62	1.386(9)	C9B	C10B	1.391(10)
C62	C63	1.399(8)	C10A	C11A	1.411(9)
C62	C65	1.474(10)	C10B	C11B	1.410(10)
B1	C66A	1.688(12)	C11A	C12A	1.406(9)
B1	C66B	1.665(14)	C11B	C12B	1.392(10)
B1	C74A	1.531(14)	C043	C74A	1.381(9)
B1	C74B	1.77(2)	C043	C78A	1.380(9)
F13A	C72A	1.344(9)	C66A	C67A	1.393(9)

F13B	C72B	1.341(10)		C66A	C71A	1.393(8)	
F14A	C72A	1.348(9)		C66B	C67B	1.40(2)	
F14B	C72B	1.346(10)		C66B	C71B	1.401(9)	
F15A	C72A	1.339(9)		C67A	C68A	1.395(9)	
F15B	C72B	1.362(10)		C67B	C68B	1.392(10)	
F16A	C73A	1.330(9)		C68A	C69A	1.387(8)	
F16B	C73B	1.349(10)		C68A	C72A	1.489(9)	
F17A	C73A	1.328(9)		C68B	C69B	1.388(10)	
F17B	C73B	1.334(9)		C68B	C72B	1.45(2)	
F18A	C73A	1.339(9)		C69A	C70A	1.378(8)	
F18B	C73B	1.340(9)		C69B	C70B	1.398(10)	
F19A	C79A	1.322(9)		C70A	C71A	1.394(8)	
F19B	C80B	1.342(9)		C70A	C73A	1.496(9)	
F20A	C79A	1.343(9)		C70B	C71B	1.404(9)	
F20B	C80B	1.344(9)		C70B	C73B	1.469(19)	
F21A	C79A	1.336(9)		C74A	C75A	1.393(9)	
F21B	C80B	1.335(9)		C74B	C75B	1.398(10)	
F22A	C80A	1.351(9)		C74B	C79B	1.396(10)	
F22B	C81B	1.347(10)		C75A	C76A	1.380(9)	
F23A	C80A	1.335(9)		C75B	C76B	1.396(10)	
F23B	C81B	1.347(10)		C76A	C77A	1.377(9)	
F24A	C80A	1.340(9)		C76A	C79A	1.506(9)	
F24B	C81B	1.330(10)		C76B	C77B	1.399(10)	
F25	C87	1.315(9)		C76B	C80B	1.40(2)	
F26	C87	1.344(10)		C77A	C78A	1.372(9)	
F27	C87	1.316(8)		C77B	C78B	1.398(9)	
F28	C88	1.329(7)		C78A	C80A	1.503(9)	
F29	C88	1.341(8)		C78B	C79B	1.393(10)	
F30	C88	1.335(7)		C78B	C81B	1.47(2)	

[1]1-X,2-Y,-Z

Table S3. Bond Angles for pentacenequinone⊂**C-2**.

Atom	Atom	Atom	Angle/°	Atom	Atom	Atom	Angle/°
N1	Pd1	N3[1]	178.77(17)	F38	C103	F37	104.3(4)
N1	Pd1	N4	91.32(16)	F38	C103	C99	113.1(4)
N3[1]	Pd1	N4	89.91(17)	F39	C103	F37	105.9(4)
N6[1]	Pd1	N1	88.29(17)	F39	C103	F38	107.6(4)
N6[1]	Pd1	N3[1]	90.48(17)	F39	C103	C99	113.5(4)
N6[1]	Pd1	N4	178.91(15)	F40	C104	F41	109.3(6)
C1	N1	Pd1	118.9(3)	F40	C104	F42	104.6(7)
C5	N1	Pd1	121.8(3)	F40	C104	C101	113.8(5)
C5	N1	C1	119.2(4)	F41	C104	C101	111.1(6)
C16	N3	Pd1[1]	120.3(3)	F42	C104	F41	104.6(6)
C16	N3	C17	119.6(4)	F42	C104	C101	112.8(5)
C17	N3	Pd1[1]	120.1(3)	C106	C105	B2	125.2(5)
C20	N4	Pd1	119.9(3)	C110	C105	C106	115.9(5)
C20	N4	C24	117.9(5)	C110	C105	B2	118.9(5)
C24	N4	Pd1	122.2(4)	C105	C106	C107	121.6(6)
C31	N5	C27	116.5(5)	C106	C107	C111	117.7(6)
C35	N6	Pd1[1]	118.7(3)	C108	C107	C106	120.9(6)
C36	N6	Pd1[1]	121.8(4)	C108	C107	C111	121.3(6)
C36	N6	C35	119.2(5)	C107	C108	C109	118.3(5)
N1	C1	C2	121.8(4)	C108	C109	C110	120.6(6)
C1	C2	C3	119.1(4)	C108	C109	C112	121.3(6)
C1	C2	C6	118.9(4)	C110	C109	C112	118.0(6)
C3	C2	C6	122.0(4)	C109	C110	C105	122.6(6)
C4	C3	C2	117.9(5)	F43	C111	C107	113.2(6)
C5	C4	C3	120.6(5)	F44	C111	F43	103.7(7)
N1	C5	C4	121.4(4)	F44	C111	F45	108.5(7)
C7	C6	C2	179.1(7)	F44	C111	C107	113.1(6)
C6	C7	C8A	173.2(7)	F45	C111	F43	104.9(6)

C6	C7	C8B	162.1(10)
C14	C13	C12A	173.0(9)
C14	C13	C12B	162.8(10)
C13	C14	C15	179.2(8)
C16	C15	C14	120.5(4)
C16	C15	C19	118.4(4)
C19	C15	C14	121.1(4)
N3	C16	C15	122.1(4)
N3	C17	C18	121.5(4)
C19	C18	C17	120.4(4)
C18	C19	C15	118.1(4)
N4	C20	C21	123.3(5)
C20	C21	C22	118.2(5)
C20	C21	C25	119.9(5)
C22	C21	C25	121.8(6)
C23	C22	C21	119.0(6)
C22	C23	C24	120.2(5)
N4	C24	C23	121.4(6)
C26	C25	C21	175.0(7)
C25	C26	C27	177.6(6)
N5	C27	C26	115.8(5)
N5	C27	C28	123.7(6)
C28	C27	C26	120.6(5)
C29	C28	C27	118.5(6)
C28	C29	C30	119.4(7)
C31	C30	C29	118.0(7)
N5	C31	C30	123.9(6)
N5	C31	C32	115.9(6)
C30	C31	C32	120.2(6)
C33	C32	C31	177.9(8)
C32	C33	C34	176.0(8)
C35	C34	C33	119.8(5)
C35	C34	C38	118.5(6)
C38	C34	C33	121.7(6)
N6	C35	C34	121.7(5)
N6	C36	C37	121.8(6)
C36	C37	C38	119.7(6)
C37	C38	C34	119.0(7)
Cl1	C113	Cl2	110.9(5)
C51	C50	C55	115.9(7)
C51	C50	B1	123.9(7)
C55	C50	B1	119.9(5)
C52	C51	C50	122.3(8)
C51	C52	C53	121.1(8)
C51	C52	C56	119.8(11)
C53	C52	C56	119.1(10)
C54	C53	C52	117.3(8)
C53	C54	C57	118.0(8)
C55	C54	C53	121.5(8)
C55	C54	C57	120.5(8)
C54	C55	C50	121.9(7)
F1	C56	F3	104.6(11)
F1	C56	C52	111.7(14)
F2	C56	F1	106.3(15)
F2	C56	F3	106.9(13)
F2	C56	C52	114.4(11)
F3	C56	C52	112.3(14)
F4	C57	C54	113.7(7)
F5	C57	F4	106.3(10)
F5	C57	F6	107.0(7)
F5	C57	C54	113.7(8)
F6	C57	F4	104.1(8)
F6	C57	C54	111.4(10)
C59	C58	B1	122.6(5)
C63	C58	C59	116.1(5)
F45	C111	C107	112.8(7)
F46B	C112	C109	105.3(12)
F47B	C112	F46B	108(2)
F47B	C112	C109	104.6(19)
F48B	C112	F46B	98.6(14)
F48B	C112	F47B	121(2)
F48B	C112	C109	117.4(9)
F46A	C112	C109	116.7(10)
F46A	C112	F48A	111.4(11)
F47A	C112	C109	115.0(12)
F47A	C112	F46A	105.0(14)
F47A	C112	F48A	100.7(15)
F48A	C112	C109	106.8(8)
C81	B2	C89	109.9(4)
C97	B2	C81	109.5(4)
C97	B2	C89	109.6(4)
C97	B2	C105	107.6(4)
C105	B2	C81	109.4(4)
C105	B2	C89	110.8(4)
O1	C39	C40	120.9(4)
O1	C39	C41^{1}	121.0(4)
C40	C39	C41^{1}	118.1(4)
C41	C40	C39	120.7(4)
C45	C40	C39	120.1(4)
C45	C40	C41	119.2(4)
C40	C41	C39^{1}	121.2(4)
C42	C41	C39^{1}	119.4(4)
C42	C41	C40	119.4(5)
C41	C42	C43	121.9(4)
C42	C43	C44	118.5(4)
C42	C43	C49	122.5(5)
C49	C43	C44	119.1(5)
C45	C44	C43	118.7(5)
C45	C44	C46	122.0(5)
C46	C44	C43	119.3(5)
C40	C45	C44	122.3(4)
C47	C46	C44	119.9(5)
C46	C47	C48	120.8(6)
C49	C48	C47	121.1(5)
C48	C49	C43	119.8(5)
C12B	N0AA	C8B	117(3)
C8A	N2A	C12A	117.8(16)
N2A	C8A	C7	113.9(11)
N2A	C8A	C9A	125.9(12)
C9A	C8A	C7	119.6(8)
C7	C8B	N0AA	108.2(16)
C9B	C8B	C7	122.3(14)
C9B	C8B	N0AA	123(2)
C10A	C9A	C8A	116.4(9)
C8B	C9B	C10B	116.2(18)
C9A	C10A	C11A	119.9(11)
C9B	C10B	C11B	118(2)
C12A	C11A	C10A	120.4(12)
C12B	C11B	C10B	125(3)
N2A	C12A	C13	118.0(10)
N2A	C12A	C11A	119.6(13)
C11A	C12A	C13	118.1(9)
N0AA	C12B	C13	111.5(19)
N0AA	C12B	C11B	121(3)
C11B	C12B	C13	113.6(14)
C78A	C043	C74A	120.0(11)
C67A	C66A	B1	123.4(8)
C67A	C66A	C71A	119.5(8)
C71A	C66A	B1	117.1(8)
C67B	C66B	B1	113.9(10)

C63	C58	B1	120.9(6)
C58	C59	C60	121.8(6)
C59	C60	C64	117.2(6)
C61	C60	C59	121.9(6)
C61	C60	C64	120.6(6)
C60	C61	C62	117.1(6)
C61	C62	C63	120.7(6)
C61	C62	C65	118.1(6)
C63	C62	C65	121.2(6)
C58	C63	C62	122.5(6)
F7	C64	C60	115.8(8)
F8	C64	F7	100.8(7)
F8	C64	C60	113.8(7)
F9	C64	F7	97.7(7)
F9	C64	F8	108.8(7)
F9	C64	C60	117.7(6)
F10	C65	F11	101.9(6)
F10	C65	F12	110.5(8)
F10	C65	C62	114.9(9)
F11	C65	C62	110.4(8)
F12	C65	F11	101.3(9)
F12	C65	C62	116.1(6)
C50	B1	C58	112.4(6)
C50	B1	C66A	104.0(6)
C50	B1	C66B	118.6(6)
C50	B1	C74B	101.4(7)
C58	B1	C66A	97.8(5)
C58	B1	C66B	109.3(6)
C58	B1	C74B	107.6(7)
C74A	B1	C50	105.1(6)
C74A	B1	C58	115.1(6)
C82	C81	C86	115.2(5)
C82	C81	B2	123.9(5)
C86	C81	B2	120.8(5)
C83	C82	C81	122.4(5)
C82	C83	C87	117.9(6)
C84	C83	C82	121.3(6)
C84	C83	C87	120.8(6)
C83	C84	C85	117.7(5)
C84	C85	C88	121.2(5)
C86	C85	C84	120.4(5)
C86	C85	C88	118.4(5)
C85	C86	C81	122.9(5)
F25	C87	F26	103.6(7)
F25	C87	F27	108.8(7)
F25	C87	C83	112.8(7)
F26	C87	C83	111.7(6)
F27	C87	F26	105.5(7)
F27	C87	C83	113.7(6)
F28	C88	F29	107.2(5)
F28	C88	F30	107.6(5)
F28	C88	C85	112.9(5)
F29	C88	C85	111.5(5)
F30	C88	F29	105.3(6)
F30	C88	C85	112.0(5)
C90	C89	B2	121.9(5)
C94	C89	C90	114.6(5)
C94	C89	B2	123.6(5)
C91	C90	C89	122.3(5)
C90	C91	C95	118.5(5)
C92	C91	C90	121.4(5)
C92	C91	C95	120.1(5)
C91	C92	C93	117.1(5)
C92	C93	C96	119.6(5)
C94	C93	C92	121.5(5)

C67B	C66B	C71B	116.1(12)
C71B	C66B	B1	129.9(11)
C66A	C67A	C68A	120.2(8)
C68B	C67B	C66B	119.9(16)
C67A	C68A	C72A	117.1(10)
C69A	C68A	C67A	119.8(8)
C69A	C68A	C72A	123.0(11)
C67B	C68B	C72B	121.2(15)
C69B	C68B	C67B	125.5(16)
C69B	C68B	C72B	112.8(12)
C70A	C69A	C68A	120.2(7)
C68B	C69B	C70B	114.1(15)
C69A	C70A	C71A	120.5(7)
C69A	C70A	C73A	116.7(10)
C71A	C70A	C73A	122.8(10)
C69B	C70B	C71B	122.1(14)
C69B	C70B	C73B	118.7(11)
C71B	C70B	C73B	119.1(12)
C66A	C71A	C70A	119.8(7)
C66B	C71B	C70B	122.3(13)
F13A	C72A	F14A	103.1(9)
F13A	C72A	C68A	116.3(14)
F14A	C72A	C68A	110.8(13)
F15A	C72A	F13A	103.1(9)
F15A	C72A	F14A	102.2(9)
F15A	C72A	C68A	119.2(14)
F13B	C72B	F14B	102.2(10)
F13B	C72B	F15B	102.3(10)
F13B	C72B	C68B	115.3(13)
F14B	C72B	F15B	101.1(9)
F14B	C72B	C68B	116.9(13)
F15B	C72B	C68B	116.7(14)
F16A	C73A	F18A	103.6(9)
F16A	C73A	C70A	113.8(12)
F17A	C73A	F16A	105.3(9)
F17A	C73A	F18A	103.8(8)
F17A	C73A	C70A	114.0(11)
F18A	C73A	C70A	115.1(11)
F16B	C73B	C70B	117.3(11)
F17B	C73B	F16B	102.4(9)
F17B	C73B	F18B	104.5(9)
F17B	C73B	C70B	115.9(11)
F18B	C73B	F16B	102.0(9)
F18B	C73B	C70B	112.9(12)
C043	C74A	B1	123.3(8)
C043	C74A	C75A	116.7(11)
C75A	C74A	B1	119.7(9)
C75B	C74B	B1	122.5(13)
C79B	C74B	B1	120.4(12)
C79B	C74B	C75B	117.1(17)
C76A	C75A	C74A	122.1(11)
C76B	C75B	C74B	124.3(16)
C75A	C76A	C79A	118.2(10)
C77A	C76A	C75A	121.0(10)
C77A	C76A	C79A	120.8(9)
C75B	C76B	C77B	117.5(15)
C75B	C76B	C80B	124.6(13)
C77B	C76B	C80B	117.9(12)
C78A	C77A	C76A	116.4(11)
C78B	C77B	C76B	119.3(15)
C043	C78A	C80A	118.5(10)
C77A	C78A	C043	123.6(11)
C77A	C78A	C80A	117.9(10)
C77B	C78B	C81B	120.3(12)
C79B	C78B	C77B	122.1(15)

C94	C93	C96	118.9(5)	C79B	C78B	C81B	117.6(13)
C93	C94	C89	123.2(5)	F19A	C79A	F20A	105.3(8)
F31	C95	F32	105.4(5)	F19A	C79A	F21A	105.4(8)
F31	C95	C91	112.0(5)	F19A	C79A	C76A	114.7(9)
F32	C95	C91	112.0(5)	F20A	C79A	C76A	111.9(9)
F33	C95	F31	107.0(5)	F21A	C79A	F20A	104.5(8)
F33	C95	F32	107.2(6)	F21A	C79A	C76A	114.0(9)
F33	C95	C91	112.8(5)	C78B	C79B	C74B	119.8(16)
F34	C96	F35	108.2(6)	F22A	C80A	C78A	116.5(10)
F34	C96	F36	108.5(5)	F23A	C80A	F22A	103.0(8)
F34	C96	C93	112.9(5)	F23A	C80A	F24A	104.3(8)
F35	C96	C93	110.1(5)	F23A	C80A	C78A	115.1(11)
F36	C96	F35	102.9(5)	F24A	C80A	F22A	103.0(8)
F36	C96	C93	113.7(5)	F24A	C80A	C78A	113.4(10)
C98	C97	C102	116.0(5)	F19B	C80B	F20B	102.7(9)
C98	C97	B2	125.1(4)	F19B	C80B	C76B	112.3(11)
C102	C97	B2	118.9(4)	F20B	C80B	C76B	115.3(11)
C99	C98	C97	122.1(5)	F21B	C80B	F19B	103.7(9)
C98	C99	C100	121.4(5)	F21B	C80B	F20B	104.1(9)
C98	C99	C103	120.1(4)	F21B	C80B	C76B	117.1(11)
C100	C99	C103	118.4(5)	F22B	C81B	C78B	111.7(11)
C99	C100	C101	116.8(5)	F23B	C81B	F22B	102.8(9)
C100	C101	C104	120.1(5)	F23B	C81B	C78B	115.6(11)
C102	C101	C100	121.6(5)	F24B	C81B	F22B	104.3(10)
C102	C101	C104	118.2(5)	F24B	C81B	F23B	103.4(9)
C101	C102	C97	122.1(5)	F24B	C81B	C78B	117.5(12)
F37	C103	C99	111.9(4)				

[1]1-X,2-Y,-Z

Table S4. Torsion Angles for pentacenequinone⊂**C-2**.

A	B	C	D	Angle/°	A	B	C	D	Angle/°
Pd1	N1	C1	C2	-177.1(4)	C97	C98	C99	C103	-177.7(5)
Pd1	N1	C5	C4	178.2(4)	C98	C97	C102	C101	0.8(8)
Pd1[1]	N3	C16	C15	179.4(4)	C98	C97	B2	C81	14.9(7)
Pd1[1]	N3	C17	C18	-179.8(4)	C98	C97	B2	C89	-105.7(6)
Pd1	N4	C20	C21	175.3(4)	C98	C97	B2	C105	133.8(5)
Pd1	N4	C24	C23	-175.6(5)	C98	C99	C100	C101	0.2(8)
Pd1[1]	N6	C35	C34	-170.3(5)	C98	C99	C103	F37	80.2(6)
Pd1[1]	N6	C36	C37	172.1(7)	C98	C99	C103	F38	-37.2(7)
N1	C1	C2	C3	-1.4(8)	C98	C99	C103	F39	-160.1(5)
N1	C1	C2	C6	179.9(5)	C99	C100	C101	C102	1.6(9)
N3	C17	C18	C19	-0.1(9)	C99	C100	C101	C104	-175.0(6)
N4	C20	C21	C22	1.9(8)	C100	C99	C103	F37	-96.0(6)
N4	C20	C21	C25	-174.8(5)	C100	C99	C103	F38	146.6(5)
N5	C27	C28	C29	-1.2(10)	C100	C99	C103	F39	23.7(7)
N6	C36	C37	C38	-1.7(14)	C100	C101	C102	C97	-2.2(9)
C1	N1	C5	C4	1.3(8)	C100	C101	C104	F40	8.2(10)
C1	C2	C3	C4	1.8(8)	C100	C101	C104	F41	-115.7(7)
C2	C3	C4	C5	-0.7(9)	C100	C101	C104	F42	127.2(7)
C3	C4	C5	N1	-0.9(9)	C102	C97	C98	C99	1.1(8)
C5	N1	C1	C2	-0.1(7)	C102	C97	B2	C81	-167.0(5)
C6	C2	C3	C4	-179.6(5)	C102	C97	B2	C89	72.4(6)
C6	C7	C8B	N0AA	132(2)	C102	C97	B2	C105	-48.1(7)
C6	C7	C8B	C9B	-75(3)	C102	C101	C104	F40	-168.5(6)
C7	C8A	C9A	C10A	170.9(8)	C102	C101	C104	F41	67.6(8)
C7	C8B	C9B	C10B	-149.0(15)	C102	C101	C104	F42	-49.5(9)
C14	C13	C12B	N0AA	113(3)	C103	C99	C100	C101	176.3(5)
C14	C13	C12B	C11B	-107(4)	C104	C101	C102	C97	174.5(6)
C14	C15	C16	N3	179.7(6)	C105	C106	C107	C108	-0.3(10)
C14	C15	C19	C18	-179.6(6)	C105	C106	C107	C111	179.6(6)
C16	N3	C17	C18	0.2(8)	C106	C105	C110	C109	2.3(9)

C16	C15	C19	C18	-0.9(9)
C17	N3	C16	C15	-0.7(8)
C17	C18	C19	C15	0.5(9)
C19	C15	C16	N3	1.0(9)
C20	N4	C24	C23	1.9(8)
C20	C21	C22	C23	-1.2(9)
C21	C22	C23	C24	1.0(10)
C22	C23	C24	N4	-1.3(10)
C24	N4	C20	C21	-2.2(7)
C25	C21	C22	C23	175.4(6)
C26	C27	C28	C29	179.6(6)
C27	N5	C31	C30	-0.9(9)
C27	N5	C31	C32	-179.6(5)
C27	C28	C29	C30	1.2(11)
C28	C29	C30	C31	-1.1(11)
C29	C30	C31	N5	0.9(11)
C29	C30	C31	C32	179.6(7)
C31	N5	C27	C26	-179.8(5)
C31	N5	C27	C28	1.0(9)
C33	C34	C35	N6	175.1(6)
C33	C34	C38	C37	-178.1(9)
C35	N6	C36	C37	-1.3(10)
C35	C34	C38	C37	-0.7(14)
C36	N6	C35	C34	3.3(8)
C36	C37	C38	C34	2.6(16)
C38	C34	C35	N6	-2.3(10)
C50	C51	C52	C53	0.1(13)
C50	C51	C52	C56	178.7(11)
C50	B1	C66A	C67A	-35.7(8)
C50	B1	C66A	C71A	147.7(6)
C50	B1	C66B	C67B	-60.5(11)
C50	B1	C66B	C71B	123.8(12)
C50	B1	C74A	C043	88.4(11)
C50	B1	C74A	C75A	-85.1(10)
C50	B1	C74B	C75B	-78.9(10)
C50	B1	C74B	C79B	100.2(8)
C51	C50	C55	C54	2.6(9)
C51	C50	B1	C58	-138.9(6)
C51	C50	B1	C66A	-34.2(9)
C51	C50	B1	C66B	-9.6(10)
C51	C50	B1	C74A	95.2(8)
C51	C50	B1	C74B	106.4(8)
C51	C52	C53	C54	1.3(13)
C51	C52	C56	F1	53.5(16)
C51	C52	C56	F2	-67(2)
C51	C52	C56	F3	170.7(12)
C52	C53	C54	C55	-0.7(12)
C52	C53	C54	C57	178.2(8)
C53	C52	C56	F1	-127.9(13)
C53	C52	C56	F2	111.4(15)
C53	C52	C56	F3	-11(2)
C53	C54	C55	C50	-1.3(11)
C53	C54	C57	F4	-162.0(7)
C53	C54	C57	F5	-40.3(13)
C53	C54	C57	F6	80.7(9)
C55	C50	C51	C52	-2.0(10)
C55	C50	B1	C58	47.3(8)
C55	C50	B1	C66A	152.0(6)
C55	C50	B1	C66B	176.5(7)
C55	C50	B1	C74A	-78.7(8)
C55	C50	B1	C74B	-67.4(8)
C55	C54	C57	F4	16.8(11)
C55	C54	C57	F5	138.6(9)
C55	C54	C57	F6	-100.4(10)
C56	C52	C53	C54	-177.3(11)
C106	C105	B2	C81	-104.2(6)
C106	C105	B2	C89	17.1(8)
C106	C105	B2	C97	136.9(6)
C106	C107	C108	C109	0.2(11)
C106	C107	C111	F43	61.7(9)
C106	C107	C111	F44	-55.9(9)
C106	C107	C111	F45	-179.4(7)
C107	C108	C109	C110	1.2(11)
C107	C108	C109	C112	178.6(7)
C108	C107	C111	F43	-118.4(8)
C108	C107	C111	F44	124.0(8)
C108	C107	C111	F45	0.5(11)
C108	C109	C110	C105	-2.6(11)
C108	C109	C112	F46B	126.9(15)
C108	C109	C112	F47B	13(2)
C108	C109	C112	F48B	-124.6(17)
C108	C109	C112	F46A	151.1(14)
C108	C109	C112	F47A	27.4(17)
C108	C109	C112	F48A	-83.5(13)
C110	C105	C106	C107	-0.9(9)
C110	C105	B2	C81	74.0(6)
C110	C105	B2	C89	-164.7(5)
C110	C105	B2	C97	-44.9(7)
C110	C109	C112	F46B	-55.7(14)
C110	C109	C112	F47B	-170(2)
C110	C109	C112	F48B	52.8(18)
C110	C109	C112	F46A	-31.5(15)
C110	C109	C112	F47A	-155.2(15)
C110	C109	C112	F48A	93.9(12)
C111	C107	C108	C109	-179.7(7)
C112	C109	C110	C105	-180.0(6)
B2	C81	C82	C83	-173.0(5)
B2	C81	C86	C85	173.6(5)
B2	C89	C90	C91	179.1(4)
B2	C89	C94	C93	180.0(4)
B2	C97	C98	C99	179.3(5)
B2	C97	C102	C101	-177.5(5)
B2	C105	C106	C107	177.4(6)
B2	C105	C110	C109	-176.1(6)
O1	C39	C40	C41	179.6(4)
O1	C39	C40	C45	0.9(7)
C39	C40	C41	C39[1]	0.5(7)
C39	C40	C41	C42	179.5(4)
C39	C40	C45	C44	179.5(4)
C39[1]	C41	C42	C43	-179.0(5)
C40	C41	C42	C43	1.9(7)
C41[1]	C39	C40	C41	-0.4(7)
C41[1]	C39	C40	C45	-179.1(4)
C41	C40	C45	C44	0.8(7)
C41	C42	C43	C44	-1.0(8)
C41	C42	C43	C49	178.6(5)
C42	C43	C44	C45	0.0(7)
C42	C43	C44	C46	179.3(5)
C42	C43	C49	C48	-178.3(6)
C43	C44	C45	C40	0.1(8)
C43	C44	C46	C47	-1.5(8)
C44	C43	C49	C48	1.3(9)
C44	C46	C47	C48	2.3(10)
C45	C40	C41	C39[1]	179.2(4)
C45	C40	C41	C42	-1.8(7)
C45	C44	C46	C47	177.8(6)
C46	C44	C45	C40	-179.2(5)
C46	C47	C48	C49	-1.3(11)
C47	C48	C49	C43	-0.5(11)
C49	C43	C44	C45	-179.6(5)

C57	C54	C55	C50	179.8(7)
C58	C59	C60	C61	-0.7(12)
C58	C59	C60	C64	-174.5(7)
C58	B1	C66A	C67A	79.9(7)
C58	B1	C66A	C71A	-96.7(7)
C58	B1	C66B	C67B	70.1(10)
C58	B1	C66B	C71B	-105.5(13)
C58	B1	C74A	C043	-35.9(13)
C58	B1	C74A	C75A	150.6(9)
C58	B1	C74B	C75B	162.9(8)
C58	B1	C74B	C79B	-18.1(10)
C59	C58	C63	C62	-2.1(10)
C59	C58	B1	C50	27.4(8)
C59	C58	B1	C66A	-81.2(8)
C59	C58	B1	C66B	-106.4(8)
C59	C58	B1	C74A	147.8(7)
C59	C58	B1	C74B	138.3(8)
C59	C60	C61	C62	-0.6(12)
C59	C60	C64	F7	54.4(10)
C59	C60	C64	F8	-61.8(11)
C59	C60	C64	F9	169.3(8)
C60	C61	C62	C63	0.5(12)
C60	C61	C62	C65	-179.2(9)
C61	C60	C64	F7	-119.5(9)
C61	C60	C64	F8	124.3(9)
C61	C60	C64	F9	-4.6(13)
C61	C62	C63	C58	0.9(12)
C61	C62	C65	F10	-59.0(12)
C61	C62	C65	F11	55.5(11)
C61	C62	C65	F12	170.0(9)
C63	C58	C59	C60	1.9(10)
C63	C58	B1	C50	-160.3(6)
C63	C58	B1	C66A	91.0(7)
C63	C58	B1	C66B	65.8(9)
C63	C58	B1	C74A	-39.9(9)
C63	C58	B1	C74B	-49.4(9)
C63	C62	C65	F10	121.3(9)
C63	C62	C65	F11	-124.2(8)
C63	C62	C65	F12	-9.7(15)
C64	C60	C61	C62	173.0(8)
C65	C62	C63	C58	-179.4(8)
B1	C50	C51	C52	-176.1(7)
B1	C50	C55	C54	176.9(6)
B1	C58	C59	C60	174.5(6)
B1	C58	C63	C62	-174.8(7)
B1	C66A	C67A	C68A	-176.7(8)
B1	C66A	C71A	C70A	177.0(8)
B1	C66B	C67B	C68B	-177.4(11)
B1	C66B	C71B	C70B	178.1(11)
B1	C74A	C75A	C76A	178.1(10)
B1	C74B	C75B	C76B	179.0(12)
B1	C74B	C79B	C78B	-178.9(12)
C81	C82	C83	C84	-1.6(9)
C81	C82	C83	C87	-179.6(6)
C82	C81	C86	C85	-2.1(8)
C82	C81	B2	C89	-142.7(5)
C82	C81	B2	C97	96.9(6)
C82	C81	B2	C105	-20.8(7)
C82	C83	C84	C85	0.2(9)
C82	C83	C87	F25	-48.4(9)
C82	C83	C87	F26	67.8(9)
C82	C83	C87	F27	-172.9(6)
C83	C84	C85	C86	0.2(8)
C83	C84	C85	C88	-179.7(5)
C84	C83	C87	F25	133.5(7)
C49	C43	C44	C46	-0.3(8)
N0AA	C8B	C9B	C10B	-0.3(3)
N2A	C8A	C9A	C10A	0.03(11)
C8A	N2A	C12A	C13	-156.5(11)
C8A	N2A	C12A	C11A	-0.1(4)
C8A	C9A	C10A	C11A	0.1(4)
C8B	N0AA	C12B	C13	136.6(15)
C8B	N0AA	C12B	C11B	-0.5(6)
C8B	C9B	C10B	C11B	0.8(6)
C9A	C10A	C11A	C12A	-0.2(7)
C9B	C10B	C11B	C12B	-1.2(8)
C10A	C11A	C12A	C13	156.6(11)
C10A	C11A	C12A	N2A	0.3(7)
C10B	C11B	C12B	C13	-135.2(16)
C10B	C11B	C12B	N0AA	1.1(9)
C12A	N2A	C8A	C7	-171.3(7)
C12A	N2A	C8A	C9A	-0.01(16)
C12B	N0AA	C8B	C7	152.6(13)
C12B	N0AA	C8B	C9B	0.1(3)
C043	C74A	C75A	C76A	4.1(17)
C043	C78A	C80A	F22A	19.1(17)
C043	C78A	C80A	F23A	-101.7(14)
C043	C78A	C80A	F24A	138.3(12)
C66A	C67A	C68A	C69A	0.0(3)
C66A	C67A	C68A	C72A	175.2(11)
C66B	C67B	C68B	C69B	-0.7(18)
C66B	C67B	C68B	C72B	170.5(16)
C67A	C66A	C71A	C70A	0.3(6)
C67A	C68A	C69A	C70A	0.0(6)
C67A	C68A	C72A	F13A	17.8(16)
C67A	C68A	C72A	F14A	135.1(10)
C67A	C68A	C72A	F15A	-106.8(13)
C67B	C66B	C71B	C70B	2.5(18)
C67B	C68B	C69B	C70B	1(2)
C67B	C68B	C72B	F13B	15(2)
C67B	C68B	C72B	F14B	134.9(13)
C67B	C68B	C72B	F15B	-105.3(16)
C68A	C69A	C70A	C71A	0.2(9)
C68A	C69A	C70A	C73A	177.9(11)
C68B	C69B	C70B	C71B	0(2)
C68B	C69B	C70B	C73B	-176.0(14)
C69A	C68A	C72A	F13A	-167.2(11)
C69A	C68A	C72A	F14A	-49.9(14)
C69A	C68A	C72A	F15A	68.3(15)
C69A	C70A	C71A	C66A	-0.3(8)
C69A	C70A	C73A	F16A	168.1(9)
C69A	C70A	C73A	F17A	47.2(13)
C69A	C70A	C73A	F18A	-72.6(12)
C69B	C68B	C72B	F13B	-172.9(14)
C69B	C68B	C72B	F14B	-52.8(19)
C69B	C68B	C72B	F15B	67.0(18)
C69B	C70B	C71B	C66B	-2(2)
C69B	C70B	C73B	F16B	118.3(15)
C69B	C70B	C73B	F17B	-3.1(19)
C69B	C70B	C73B	F18B	-123.5(14)
C71A	C66A	C67A	C68A	-0.1(3)
C71A	C70A	C73A	F16A	-14.3(15)
C71A	C70A	C73A	F17A	-135.2(11)
C71A	C70A	C73A	F18A	105.0(12)
C71B	C66B	C67B	C68B	-1.2(13)
C71B	C70B	C73B	F16B	-58.0(17)
C71B	C70B	C73B	F17B	-179.4(12)
C71B	C70B	C73B	F18B	60.1(16)
C72A	C68A	C69A	C70A	-174.9(12)
C72B	C68B	C69B	C70B	-170.7(15)

C84	C83	C87	F26	-110.2(7)	C73A	C70A	C71A	C66A	-177.9(11)
C84	C83	C87	F27	9.0(10)	C73B	C70B	C71B	C66B	174.1(12)
C84	C85	C86	C81	0.8(8)	C74A	C043	C78A	C77A	-1(2)
C84	C85	C88	F28	-6.3(8)	C74A	C043	C78A	C80A	177.1(11)
C84	C85	C88	F29	114.4(6)	C74A	C75A	C76A	C77A	-4.9(19)
C84	C85	C88	F30	-127.9(6)	C74A	C75A	C76A	C79A	175.3(11)
C86	C81	C82	C83	2.4(8)	C74B	C75B	C76B	C77B	0.0(3)
C86	C81	B2	C89	42.1(6)	C74B	C75B	C76B	C80B	179.6(13)
C86	C81	B2	C97	-78.3(6)	C75A	C76A	C77A	C78A	2.3(19)
C86	C81	B2	C105	163.9(5)	C75A	C76A	C79A	F19A	-60.4(14)
C86	C85	C88	F28	173.8(5)	C75A	C76A	C79A	F20A	59.6(14)
C86	C85	C88	F29	-65.5(7)	C75A	C76A	C79A	F21A	178.0(10)
C86	C85	C88	F30	52.2(8)	C75B	C74B	C79B	C78B	0.2(6)
C87	C83	C84	C85	178.2(6)	C75B	C76B	C77B	C78B	0.0(6)
C88	C85	C86	C81	-179.3(5)	C75B	C76B	C80B	F19B	-21.3(15)
C89	C90	C91	C92	1.1(8)	C75B	C76B	C80B	F20B	95.9(13)
C89	C90	C91	C95	179.7(5)	C75B	C76B	C80B	F21B	-141.1(11)
C90	C89	C94	C93	-0.2(7)	C76A	C77A	C78A	C043	1(2)
C90	C89	B2	C81	42.1(6)	C76A	C77A	C78A	C80A	-177.8(11)
C90	C89	B2	C97	162.5(4)	C76B	C77B	C78B	C79B	0.1(9)
C90	C89	B2	C105	-78.9(6)	C76B	C77B	C78B	C81B	-179.6(12)
C90	C91	C92	C93	-0.5(7)	C77A	C76A	C79A	F19A	119.9(13)
C90	C91	C95	F31	53.3(7)	C77A	C76A	C79A	F20A	-120.1(12)
C90	C91	C95	F32	-64.9(6)	C77A	C76A	C79A	F21A	-1.8(16)
C90	C91	C95	F33	174.0(5)	C77A	C78A	C80A	F22A	-162.3(12)
C91	C92	C93	C94	-0.4(7)	C77A	C78A	C80A	F23A	76.9(15)
C91	C92	C93	C96	179.4(4)	C77A	C78A	C80A	F24A	-43.0(16)
C92	C91	C95	F31	-128.2(5)	C77B	C76B	C80B	F19B	158.3(10)
C92	C91	C95	F32	113.7(6)	C77B	C76B	C80B	F20B	-84.5(12)
C92	C91	C95	F33	-7.4(8)	C77B	C76B	C80B	F21B	38.5(14)
C92	C93	C94	C89	0.8(7)	C77B	C78B	C79B	C74B	-0.2(9)
C92	C93	C96	F34	-125.9(6)	C77B	C78B	C81B	F22B	85.0(13)
C92	C93	C96	F35	113.1(6)	C77B	C78B	C81B	F23B	-32.1(15)
C92	C93	C96	F36	-1.7(7)	C77B	C78B	C81B	F24B	-154.7(10)
C94	C89	C90	C91	-0.7(7)	C78A	C043	C74A	B1	-174.7(11)
C94	C89	B2	C81	-138.1(5)	C78A	C043	C74A	C75A	-1.0(17)
C94	C89	B2	C97	-17.8(6)	C79A	C76A	C77A	C78A	-177.9(11)
C94	C89	B2	C105	100.8(5)	C79B	C74B	C75B	C76B	-0.1(3)
C94	C93	C96	F34	53.8(7)	C79B	C78B	C81B	F22B	-94.8(12)
C94	C93	C96	F35	-67.1(7)	C79B	C78B	C81B	F23B	148.2(10)
C94	C93	C96	F36	178.0(5)	C79B	C78B	C81B	F24B	25.6(14)
C95	C91	C92	C93	-179.1(5)	C80B	C76B	C77B	C78B	-179.7(12)
C96	C93	C94	C89	-179.0(4)	C81B	C78B	C79B	C74B	179.5(12)
C97	C98	C99	C100	-1.6(8)					

[1]1-X,2-Y,-Z

References

[S1] D. P. August, G. S. Nichol, P. J. Lusby, *Angew. Chem. Int. Ed.* **2016**, *55*, 15022–15026.

[S2] V. Martí-Centelles, A. L. Lawrence, P. J. Lusby, *J. Am. Chem. Soc.* **2018**, *140*, 2862–2868.

[S3] Timur V. Elzhov, Katharine M. Mullen, Andrej-Nikolai Spiess and Ben Bolker (2015). minpack.lm: R Interface to the Levenberg-Marquardt Nonlinear Least-Squares Algorithm Found in MINPACK, Plus Support for Bounds. R package version 1.2-0. https://CRAN.R-project.org/package=minpack.lm [Accessed 31st August 2018]

[S4] R Core Team (2015). R: A language and environment for statistical computing. R Foundation for Statistical Computing, Vienna, Austria. URL https://www.R-project.org/. [Accessed 31st August 2018]

[S5] Studio Team (2015). RStudio: Integrated Development for R, version 0.99.892. RStudio, Inc., Boston, MA URL http://www.rstudio.com/. [Accessed 31st August 2018]

[S6] Kenneth A. Connors, *Binding Constants: The Measurement of Molecular Complex Stability*. New York: John Wiley & Sons, **1987**.

[S7] Berend Hasselman (2016). nleqslv: Solve Systems of Nonlinear Equations. R package version 3.0.3. https://CRAN.R-project.org/package=nleqslv [Accessed 31st August 2018]

[S8] G. Ercolani, C. Piguet, M. Borkovec, J. Hamacek *J. Phys. Chem. B* **2007**, *111*, 12195–12203.

[S9] T. A. Young, V. Martí-Centelles, J. Wang, P. J. Lusby, F. Duarte, *J. Am. Chem. Soc.* **2019**, *in press*, **DOI**: 10.1021/jacs.9b103028.

[S10] Karline Soetaert, Thomas Petzoldt, R. Woodrow Setzer (2010). Solving Differential Equations in R: Package deSolve. Journal of Statistical Software, 33(9), 1–25. URL http://www.jstatsoft.org/v33/i09/ DOI 10.18637/jss.v033.i09 [Accessed 31st August 2018]

[S11] W. M. Getz, P. Lánsky, *Chem. Senses* **2001**, *26*, 95–104.

[S12] P. Liao, B. W. Langloss, A. M. Johnson, E. R. Knudsen, F. S. Tham, R. R. Julian, R. J. Hooley, *Chem. Commun.* **2010**, *46*, 4932–4934.

[S13] J. E. M. Lewis, E. L. Gavey, S. A. Cameron, J. D. Crowley, *Chem. Sci.* **2012**, *3*, 778–784.

[S14] J. E. M. Lewis, J. D. Crowley, *Supramol. Chem.* **2014**, *26*, 173–181.

[S15] D. Preston, J. E. M. Lewis, J. D. Crowley, *J. Am. Chem. Soc.* **2017**, *139*, 2379–2386.

[S16] A. L. Spek, *Acta Crystallogr. Sect. C Struct. Chem.* **2015**, *71*, 9–18.

[S17] O.V. Dolomanov, L. J. Bourhis, R.J Gildea, J. A. K. Howard, H. Puschmann, *J. Appl. Cryst.* **2009**, *42*, 339–341.

[S18] G.M. Sheldrick, *Acta Cryst.* **2015**, *A71*, 3–8.

[S19] G.M. Sheldrick, *Acta Cryst.* **2015**, *C71*, 3–8.